ROLE OF SREBP IN KIDNEY FIBROSIS

THE ROLE OF STEROL REGULATORY ELEMENT BINDING PROTEIN (SREBP) IN KIDNEY FIBROSIS

By MARIA MUSTAFA, B.Sc.

A Thesis Submitted to the School of Graduate Studies in Partial Fulfilment of the Requirements for the Degree Master of Science

McMaster University MASTER OF SCIENCE (2013) Hamilton, Ontario (Medical Science)

TITLE: The role of Sterol Regulatory Element Binding Protein (SREBP) in kidney fibrosis

AUTHOR: Mustafa, B.Sc. (McMaster University) SUPERVISOR: Dr. J. Krepinsky

NUMBER OF **PAGES: vii, 72**

Abstract

There has been a steady increase in the number of patients with chronic kidney disease. The etiology has been linked to excessive fibrosis progression until the kidney function becomes compromised. We are investigating tubulointerstitial fibrosis (TIF) specifically, as it correlates strongly with the decline of renal function.

In our study we investigated the role that active SREBP may play in apoptosis and fibrosis in vivo and in vitro. Treating HK-2 cells with TNFα resulted in the cleavage of SREBP and activation of its SRE promoter. By utilizing a number of inhibitors, we found TNFα induced SREBP cleavage through both a caspase independent and dependent manner.

We used fatostatin, a SCAP inhibitor, to reduce the amount of active SREBP in animals in the unilateral ureter obstruction (UUO) model. This model is well known for its development of TIF. Fatostatin decreased SREBP-1 and SREBP-2 activation in mice after 7 and 14 days. Fatostatin increased glomerulotubular integrity and proximal tubular mass as evaluated using lectin staining, along with reducing the number of cells undergoing apoptosis as evaluated by TUNEL staining. Using the Masson Trichrome, Picrosirius red and fibronectin staining, we found a reduction of fibrosis. Fatostatin was also found to attenuate the accumulation of infiltrating myofibroblasts and T cells. These results point to a pathological role for SREBP in TIF.

Acknowledgments

I would like to begin this page by thanking my parents. They have been my inspiration and hope. They have been there for me when my experiments failed, or my mice fell sick and unfortunately passed away. Their inspiring words have kept me going and will keep me going until I have achieved my dreams.

The next person I would like to thank is Dr. Joan Krepinsky for providing this incredible opportunity. Working with her, I realized anything is possible if you really work hard at it. She is my idol, someone who I aspire to be. She has helped me become a better researcher by problem solving and a better teacher to new students in the lab.

Next I would like to acknowledge those in the lab that have helped me in completing my thesis. Especially Bo Gao. She has helped me with my surgeries on every mouse, and always reassured me that the mouse will survive. You are an incredible person! Also Veronica, I have not forgot about you. I can still remember the moment when you attempted to prevent the mouse from dying by keeping it on the heating pad. I would like to thank you for providing encouraging words during my most feared IP injections and assisting on UUO. I would also like to thank Andrew Pawelka, who although is not a part of my lab, has assisted me in euthanizing mice.

I would also like to thank my committee members, Dr. Darren Bridgewater and Dr. Peter Margetts. You have both been helpful by providing a critical eye to my

research and providing solutions for the problems I have had. Let us not forget allowing me to defend and officially graduate. This is one of the best committees I have had for my thesis.

Table of Contents

List of Figures

List of Abbreviations

AEBSF	4-(2-Aminoethyl) benzenesulfonyl fluoride hydrochloride
ATG	Atubular Glomeruli
BrdU	Bromodeoxyuridine
FADD	Fas-Associated protein with Death Domain
GFP	Green Fluorescent protein
ECM	Extracellular matrix
NFkB	Nuclear factor kappa-light-chain-enhancer of activated B cells
PARP	Poly (ADP-ribose) polymerase
PSR	Picrosirius red
PTEC	Proximal Tubular Epithelial Cells
SCAP	SREBP cleavage-activating protein
αSMA	α-Smooth Muscle Actin
SRE	Sterol Regulatory Element
SREBP	Sterol Regulatory Element Binding Protein
TdT	Terminal deoxynucleotidyl transferase
TGF	Tumor Growth Factor
TIF	Tubulointerstitial fibrosis
TNF	Tumor Necrosis Factor
TNFR	TNF receptor
TRADD	TNFR associated death domain

UUO	Unilateral Ureteral Obstruction
zVAD	N-benzyloxycarbonyl-Val-Ala-Asp fluoromethyl ketone

I. Introduction

1.1 Chronic Kidney disease

Approximately 3 million Canadians were estimated to develop kidney disease in 2009. According to Statistics Canada, of those individuals, 1.8 million are diabetic and the rest have renal vascular disease, hypertension, polycystic kidney disease, high blood pressure and glomerulonephritis. Among the 40 thousand individuals treated for kidney failure, 41% were placed on the waiting list for a transplant and 59% were placed on dialysis. Of the 16.4 thousand individuals on the waiting list for an organ transplant, 80% are waiting for a kidney. In 2010, a third of these individuals passed away waiting for a kidney transplant. There is an obvious need for organs, but the likelihood of obtaining additional donors is questionable, as the need far exceeds the supply. As Benjamin Franklin once stated, "an ounce of prevention is worth a pound of cure." Thus, the next best option to explore is a more desirable prevention technique to maintain the longevity and viability of kidneys. The particular one being investigated in this study involves arresting the expansion of kidney fibrosis, specifically in the tubulointerstitial region.

1.2 Tubulointerstitial fibrosis (TIF)

Regardless of the etiology, kidney fibrosis is common to all causes of end stage renal disease. Fibrosis occurs in the glomerulus and tubulointerstitium. However, the focus of my studies is tubulointerstitial fibrosis, as its progression correlates more

strongly with the decline of renal function than that of glomerular fibrosis (Kriz and Hir, 2005)

In the tubulointerstitium, fibroblast and fibroblast-like cells, which are recruited to the area, are key in the progression of fibrosis. These α-smooth muscle actin (αSMA)-expressing fibroblast-like cells, also known as myofibroblasts, have three accepted origins (Ishii et al., 2005; Zeisberg et al., 2007). However, according to some of the recent literature findings, the most probable origin is the resident interstitial cells also known as pericytes (Kriz et al., 2011; Picard et al., 2008; Humphreys et al., 2010). These cells secrete extracellular matrix (ECM) to assist in wound healing. Some controversial findings have found the kidneys undergo fibrosis to support the healthy remaining nephrons (Koesters et al., 2010). However, those nephrons eventually degenerate as a result of impact of the increased load. As the ECM accumulates further kidney function is impaired.

1.3 Tubular cells

TIF is an obvious phenotype observed when kidneys suffer from persisting injury. According to a review article written by Kaissling et al. (2013) TIF is secondary to tubular epithelial cells (TEC) undergoing apoptosis. In this article she mentions there are two types of cells found in the proximal tubule. One is capable of regeneration (Grone et al., 1987; Smeets et al., in press) and the other incapable of

regeneration (Bonventre and Yang, 2011; Lan et al., 2012). The degree of kidney injury is dependent on the type of PTEC that undergoes cell death.

Apoptotic TEC also contribute to fibrosis by releasing cytokines such as endothelin-1 and TGFβ (Hagimoto et al., 1997; Iwano et al., 2002; Terzaghi et al., 1978). TGFβ1 is a chemoattractant for macrophage (Wahl et al., 1987) and fibroblast cells (Postlethwaite et al., 1987). The increase in TGFβ expression was found to accompany proteoglycan, fibronectin and other matrix components deposition in the Tubular interstitial space (Tomooka et al., 1992; Strutz and Zeisberg, 2006). The positive correlation between apoptosis and fibroblast accumulation was also confirmed in a study evaluating polycystic kidney disease (Woo, 1995).

1.4 Apoptosis

According to Hengartner (2000), apoptosis is defined as programmed cell death, during which cells undergo characteristic morphologic and physiologic changes. Not only is it a useful pathway to remove damaged and potentially harmful cells, it is also a process used to control the number of cells present (Arends and Wyllie, 1991). Its importance has been acknowledged in the immune system, embryonic development, metamorphosis, and chemical-induced cell death (Ellis, et al., 1991; Cohen et al., 1992).

Apoptosis can occur through the extrinsic (death receptor) and intrinsic (mitochondrial) organelle-based pathways (Green and Reed, 1998). Sterol regulatory

element binding protein (SREBP)-1 and tumor necrosis factor (TNFα), discussed further below, utilize both of these pathways to induce apoptosis (Hsu et al., 1995; Deng et al., 2003). Regardless of the pathway the cell is committed to, caspase-3 is an important protease that is activated as the final common mediator of cell death (Elmore, 2007).

1.5 TNFα and Apoptosis

During fibrosis, cells that do not reorganize their structure to adapt to the changing environment undergo apoptosis (Kim et al., 1998). Multiple cytokines including the proinflammatory TNFα have been found to actively participate in this apoptosis. The mature form of TNFα, a 157kDa homotrimeric protein, is characterized by its cachexia-inducing and tumor necrotizing properties (Sugarman et al., 1985; Creasey et al., 1987; Larrick and Wright, 1990). TNFα binds to its receptors to induce various biological actions (Loetscher et al., 1990; Schall et al., 1990). These are TNFRI and TNFR2, which are derived from separate genes (Ortiz et al., 1995).

TNFR1 has a molecular mass of 55kDa and mediates cytotoxic and proinflammatory actions, along with extrinsic cell death in response to TNFα. The most accepted method that TNFα uses to carry out its pro-apoptotic actions is by binding to this receptor and recruiting the protein TNFR associated death domain (TRADD). TNFα-TRADD complex binds to Fas-Associated protein with Death Domain (FADD) to activate caspase-8 (Chinnaiyan et al., 1995; Hsu et al., 1995; Wajant, 2002). This subsequently activates caspase-3, committing the cell to apoptosis (Ogasawara

et al., 1993). Since the TNFR1 can activate both pro- and anti-apoptotic pathways, NFκB downregulation is necessary for exclusive apoptotic stimulation. NFkB activates genes that are known as inhibitors of apoptosis. These genes directly inhibit the caspases involved in apoptosis, including caspase-3 (Roy et al., 1997; Salvesen and Duckett, 2002).

TNFR2 has a molecular mass of 75kDa and is expressed in tubular and immune cells. This receptor is found to enhance the actions of TNFR1 and is involved in the extrinsic cell death pathway. TNFR2 is usually upregulated when TNFα cytokine levels decrease as a way to pass the ligand to TNFR1 (Zheng et al., 1995; Pimentel-Muinos and Seed, 1999). It also functions to enhance TNFR1-induced apoptosis by suppressing NFκB (Deveraux and Reed, 1999; Salvesen and Duckett, 2002). It does so by ubiquitin-dependent degradation of TRAF2, thereby interfering with TRADD upregulation of NFκB (Li et al., 2002). Co-stimulation of both receptors is necessary for increased cell death, as opposed to TNFR1 stimulation alone (Fotin-Mileczek et al., 2002; Tolosa et al., 2005).

These pathways explain how TNFα may induce apoptosis in various cell types. However, whether SREBP-1 regulates TNFα-induced apoptosis has not as of yet been investigated.

1.6 SREBP-1

SREBP 1a, 1c, and 2 are members of the basic-helix-loop-helix-leucine zipper (bHLH-ZIP) family of transcription factors. The inactive precursor form is found in the

endoplasmic reticulum (ER) bound to SCAP and Insig proteins. As sterol levels become depleted, SCAP undergoes a conformational change that weakens its binding to Insig, an ER resident protein, and promotes its binding to Cop II proteins. This interaction forms a vesicle to carry the SREBP/SCAP complex to the Golgi, where Site 1 Protease (S1P) and Site 2 Protease (S2P) cleave SREBP to produce the mature transcription factor (Sun et al., 2007). The active forms of SREBP 1a, c and 2 (Yokoyama et al., 1993) then travel to the nucleus and trigger transcriptional activation by binding to promoters of responsive genes. There are two primary binding sites for SREBP, namely the sterol regulatory element (SRE) and E-box. The SRE is found at the promoter region of HMG-CoA reductase, Farnesyl Pyrophosphate Synthase (FPPs), FAS and LDLR genes (Wang et al., 1994; Osbome, 2000; Shimano, 2002). SREBP 1a and 1c regulate fatty acid biosynthetic genes, while SREBP 1a and 2 regulate cholesterol regulatory genes, resulting in the increase of endogenous cholesterol and lipids level. After reaching the threshold for sterols, SREBP proteolysis is abolished. This is made possible by the binding of cholesterol to SCAP, causing its conformational change to enable binding of SCAP/ SREBP to Insig and retention in the ER (Goldstein et al., 2006).

Proteins other than sterols or cholesterol can also suppress SREBP activation. For example, 25-hydroxycholesterol has also been found to suppress SREBP cleavage by binding to Insig protein (Radhakrishnan et al., 2008). Importantly, non-sterol-mediated regulation of SREBP cleavage has also been described. For example, insulin or glucose has been shown to lead to SREBP activation. (Matsuda et al., 2001, Uttarwar

et al., 2012). This transcription factor has also been found to be upregulated in hepatic cells treated with TNFα (Lawler et al., 1998).

1.61 SREBP-1 and Apoptosis

Although SREBP can be activated during apoptosis, the cholesterol biosynthetic pathway was found to be unnecessary, as plasma lipoprotein was accessible to the apoptotic cell. Furthermore, increasing the level of sterols did not suppress apoptosis-activated SREBP cleavage, supporting the notion of sterol-independent SREBP activation (Goldstein and Brown, 1990).

SREBP is of great importance for this project because of the relationship it has with various Caspases. Caspase 1 has been found to activate SREBP in response to pore-forming toxins. Gurcel et al. (2006) demonstrated that caspase-1 acts on an intermediate protein that induces cleavage of SREBP-1 by S1P and S2P. This then causes an increase in lipogenic genes for pro-survival. Unlike caspase 1, caspase 2 is regulated by both SREBP-1c (Logette et al., 2005b) and SREBP-2 (Logette et al., 2005a). The transcription of this caspase is regulated by SREBP binding to its SRE-type promoter and its E-box site (Logette, 2005b). Interestingly, caspase 2 is believed to take part in lipid homeostasis, since it is only upregulated by SREBP 1c and 2 and not by SREBP 1a (Logette et al., 2005a).

Caspase-3 is a heterotrimeric enzyme and a member of the Interleukin-1 β-converting enzyme (ICE) family. It has been found to be upstream of SREBP, cleaving

the transcription factor at aspartate and serine residues found in the sequence SEPDSP (Fernandes-Alemri et al., 1994). This liberated SREBP-1 and 2 (Wang et al., 1996). According to Pai et al., (1996) the SREBP can be proteolytically cleaved by Caspase-3 in a manner than is distinct to the normal regulation of this transcription factor. The SREBP is then capable of binding to the SRE gene to initiate the apoptotic process, which includes initiating all phenotypic changes found in apoptosis (Wang et al., 1996). This transcription factor is known to specifically cleave gelsolin to cause morphological changes such as membrane blebbing (Kothakota et al., 1997).

The potential mechanism for SREBP-1 involvement in TNFα induced apoptosis is illustrated below.

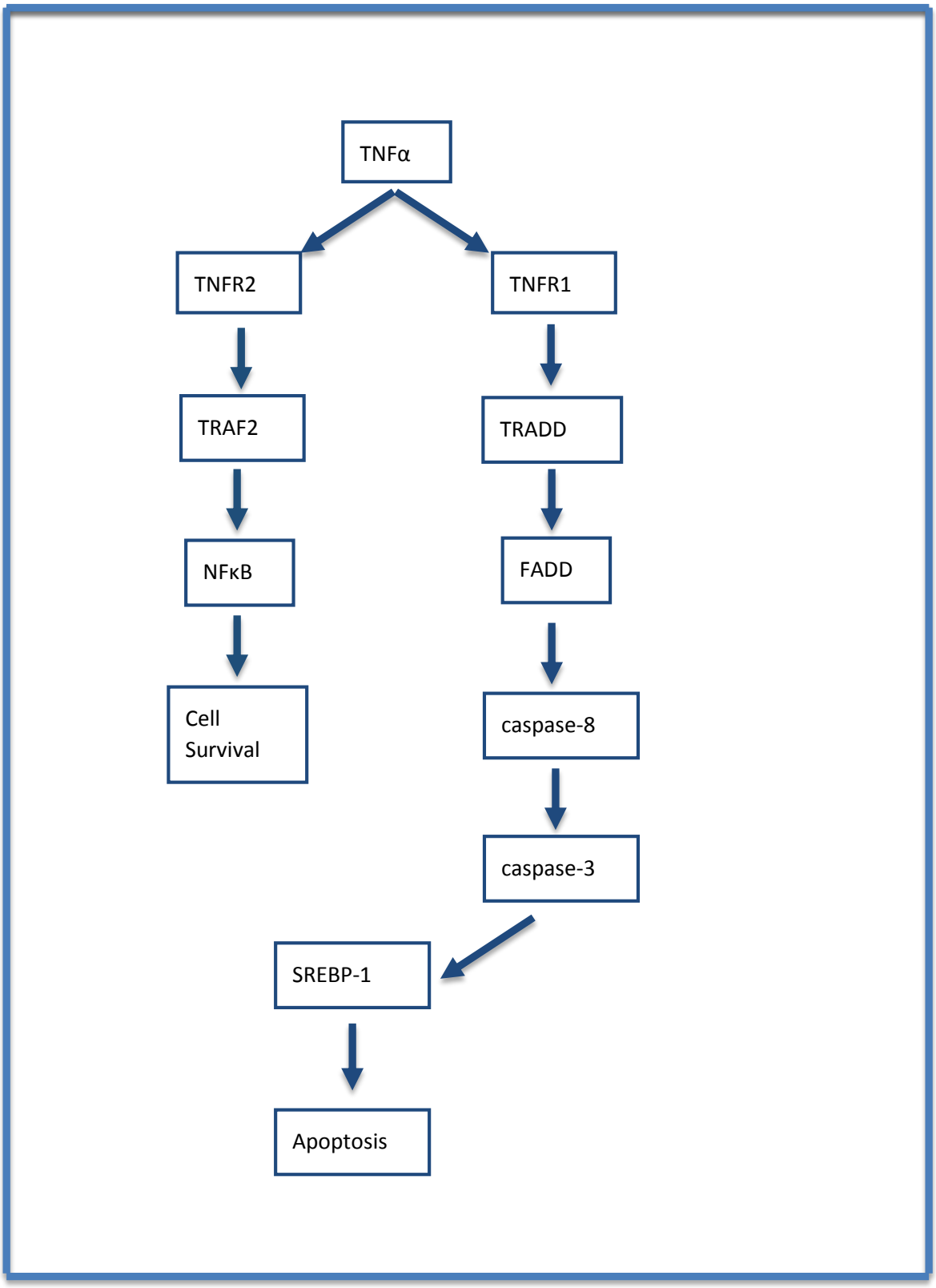
TNFα
TNFR2
TNFR1
TRAF2
TRADD
NFκB
FADD
Cell Survival
caspase-8
caspase-3
SREBP-1
Apoptosis

1.7 Recruitment of Immune Cells

Along with myofibroblast, other cells are recruited to assist in the "healing process". Often cytokines produced by tubular cells during fibrosis, such as TGFβ and TNFα attract immune cells such as monocytes/macrophages and T-cells. There is an increased amount of T-cells recruited as a result of TNFα expression, which is also known as a death cytokine according to Leornardo et al., 1999). Monocytes enter the injured area via diapedesis (Diamond, 1995) and assist in the progression of fibrosis by stimulating cells to undergo apoptosis (Lenda et al., 2003). As fibrosis persists, the blood supply is compromised, eventually leaving the fibrotic tissue hypoxic (Adamson et al., 1988).

1.8 UUO model

The specific model that will be used to evaluate fibrosis in mice is the well-established unilateral ureteral obstruction (UUO) model. UUO manifests a similar phenotype to that found in human chronic kidney disease. This includes apoptosis of tubular cells, dilation of tubules, and tubulointerstitial fibrosis (Misseri et al., 2004).

TNFα production is increased during renal obstruction and plays a role in tubulointerstitial fibrosis (Misseri et al., 2004). The role of TNFα has been evaluated in UUO using mice with deletion of either the TNFα gene or one of its receptors. Guo et al. (1999) found a decrease in UUO-induced fibrosis in mice with deletion of TNFR1 and TNFR2. This is similar to findings by Meldrum et al. (2007) who used soluble

receptors to neutralize TNFα protein levels following UUO, resulting in a decrease in fibrosis. Morimoto et al. (2008) evaluated the effects of TNFα gene deletion in chronic UUO. Unlike the findings in Meldrum et al. (2007) and Guo et al. (1999), there was an increase in fibrosis in mice lacking TNFα. The difference in outcome may be due to the lack of apoptosis of macrophages, or due to the upregulation of TNFβ, which may have similar effects to those of TNFα. TNFβ expression will not addressed in this study.

II. Hypothesis

This particular study will evaluate the involvement of SREBP in TNFα-induced apoptosis. **The hypothesis that will be evaluated in this study is that SREBP is involved in TNFα-induced apoptosis of renal tubular epithelial cells. Consequently, blocking SREBP activation will attenuate renal fibrosis.** The following Aims will be used to verify this hypothesis.

2.1 Aims

Aim 1: Does SREBP mediate TNFα-induced apoptosis in tubular cells?

Aim 2: Does SREBP inhibition attenuate apoptosis and fibrosis in vivo in the UUO model?

III. Methods and Materials

3.1 Tubular Cell Culture

A human proximal tubular epithelial cell line, HK-2, was used. These cells are immortalized proximal tubule epithelial cells (PTC) derived originally from normal adult human kidney (HK-2 cells) by exposure to a recombinant retrovirus containing the human papillomavirus (HPV) 16 E6/E7 genes. According to Ryan et al. (1994) the use of these particular cells has allowed the reproduction of experimental results obtained from primary PTC.

The cells were maintained in 10% FBS DMEM/F12 solution until the day prior to the experiment. At 90-95% confluency, cells were serum deprived overnight with 0.5% FBS. For a longer duration study, medium was changed every other day.

3.11 Transfection

SRE-GFP Transfection Assay

HK-2 cells were transfected with a green fluorescent protein (GFP) plasmid that is downstream of the sterol regulatory element (SRE) using Effectene (Qiagen). Twenty-four hours after plating of cells, they were transfected for 16 hours in 10% medium after which the medium was changed to fresh 10%. After 8 hours, the medium was changed to 0.5% FBS. Twenty-four hours later, the cells were treated for 8 hours with TNFα (10ng).

3.12 Protein Extraction/Western Blots

Cells were washed with PBS and harvested with lysis buffer containing 5μg/mL N-[N-(N-Acetyl-L-leucyl)-L-leucyl]-L-norleucine (ALLN). ALLN is a cysteine protease inhibitor that blocks the breakdown of SREBP. The lysate was then run on gels for western blots. 7.5% gels were used for SREBP, while a 12.5% gel was used to evaluate proteins at 12 and 17kDa such as the cleaved form of Caspase-3. Fifty μg of protein was used for all protein analysis excluding Tubulin for which 10μg was used. Following the transfer of the blot on a nitrocellulose membrane, Ponceau S was used to ensure all bands were transferred and each lane had the same amount of protein. The membrane was placed in 10% milk for blocking for 1 hour at room temperature. It was then incubated with primary antibody overnight in the fridge on a shaker. The following day it was washed with 1×TBS-T and incubated with secondary antibody for an hour and a half. ECL was then applied for imaging purposes.

Antibodies were used as follows at 1:1000 dilutions: SREBP-1 (Santa Cruz 8984), SREBP-2 (Santa Cruz 8151), Caspase-3 (Cell Signaling, 9665), PARP (Cell Signaling, 9542), Tubulin (Sigma, T6074), pAkt S473 (Cell Signaling, 9275S).

3.2 Animal Studies

Canadian Council on Animal Care guidelines and McMaster University approval were used to carry out the animal studies. Male 7 week old C57BL/6 Jax mice were used in this study. After acclimatization to the environment for a week, the right side of their back was shaved using an electric trimmer. The following day they

were weighed and underwent surgery. The control mice underwent sham surgery in which the ureter was left undisturbed, while the others had their right ureter ligated. The analgesic injected subcutaneously was short-term buprenorphine (Temgesic/Buprenex) (0.3mg/ml). It was recombined in saline immediately before surgery. Postoperatively mice were housed singly per cage.

3.21 Groups

Although there are four experimental groups, only two treatments were administered intraperitoneally daily with the use of a 25-gauge syringe as the mouse was restrained. The treatment commenced three days prior to surgery. The treatment mice were given fatostatin (CHEM Bridge, 5533803). This drug powder was dissolved in DMSO at the concentration of 40mg/ml and kept in 4°C fridge for a maximum of one week. Daily 150µL of drug was removed from this eppendorf tube and recombined in 1.35mL of 2/3 dextrose-1/3 NaCl solution. It was spun down and immediately administered to mice. This was the treatment for the fatostatin (Fato) group (n=3) and the UUO (UUO+Fato) (n=7) group who had their ureter ligated.

The control (Con) group (n=3) was given 150µL of DMSO recombined in 1.35mL of 2/3 dextrose-1/3 NaCl solution. This was also the treatment for the UUO group who had their ureter ligated (n=10).

3.22 Euthanasia

Following 1, 3, 7, 14 and 21 days the mice were anesthetized using isoflurane (Forane). The thoracic cavity was then opened and the hearts were perfused with 10mL of cold PBS. The kidneys were then removed from the abdomen. Following the removal of peri-renal fascia including adrenal glands, the kidneys were weighed and data was collected. The kidney was divided into three parts for immunohistochemistry (IHC), immunofluorescence (IF) and western blot samples.

3.23 Immunohistochemistry (IHC)

Processing for IHC

Kidneys sections were immersed in 10% phosphate buffered formalin overnight. They were then embedded in paraffin and sagittaly sectioned with 4uM thickness using a microtome. They were then placed on hydrophobic slides and left to dry overnight.

IHC staining

The samples were then placed in 3 changes of xylene and 2 changes of 100%ethanol followed by hydrogen peroxide and washes with ethanol, water and 1×TBS. Depending on the antibody, the samples had antigen retrieval, where they were placed in citric acid buffer for 45minutes in a rice cooker. They were washed with 1×TBS and blocking serum was placed on the samples for 15 minutes. The

primary antibody diluted in blocking serum was then applied; the time and concentration was dependent on the antibody used. The samples were washed with 1×TBS and then secondary antibody (Vector) diluted in 1×TBS was applied for 30 minutes. The concentration of the secondary antibody was dependent on the primary antibody, however mostly 1:500 concentration was used. The samples were then washed with 1×TBS and then streptavidin (Vector) diluted in 1×TBS at a concentration of 1:100 was applied. The samples were then washed with 1×TBS and then water. NOVA red (Vector labs) was applied for up to a minute, the slides were observed under the microscope and placing it in water stopped the reaction. Hemotoxylin (Sigma) was applied for 30 seconds. The slides were placed in water, ethanol, and xylene and then sealed with a coverslip and a drop of paraformaldehyde (Sigma-Aldrich).

Antibodies were used as follows with their respective concentration in 1×TBS: 1.3:100 SREBP-1 (abcam, ab44153), 1:20 SREBP-2 (Santa Cruz, 8151), 1:200 CD3 (Dako, A0452), 1:1500 α-SMA (Pierce, MAI06110), 1:200 Caspase-3 (Cell Signaling, 9664), 1:200 F4/80 (abcam, ab6640), 1:200 Fibronectin (Sigma-Aldrich, f3648).

Picrosirus red (PSR) (Polysciences, Inc.)

PSR was used in accordance to the protocol that this company provided to stain collagen I and III. The kit includes reagent A, B and C along with Weigerts hematoxylin. After the slides were deparaffinized using xylene and 100% ethanol, they were hydrated with water. Hematoxylin solution was applied for 10 seconds.

Slides were rinsed with water, then solution A was applied for 2 minutes. After another rinse with water, Solution B was applied for 1 hour and Solution C for 2 minutes. The slides were places in 70% ethanol, then dehydrated and mounted using paraformaldehyde.

TACS•symbolXL- Blue Label in Situ (TUNEL) (Trevigen)

TUNEL detects DNA fragmentation by identifying the 3'-hydroxyl ends exposed in DNA by using terminal deoxynucleotidyl transferase (TdT). This is an enzyme that catalyzes the addition of deoxyribonucleotides. The biotinylated bromodeoxyuridine (BrdU) recognizes and binds to the deoxyribonucleotides. The anti-BrdU antibody and streptavidin is then used to visualize the blue apoptotic cells.

TUNEL was used in accordance to the protocol this company provided, to stain for apoptotic cells. The samples were deparaffinized with xylene and 100% ethanol. The samples were then hydrated with 95% and 70% of ethanol. It was washed with 1xPBS then 50µL of proteinase K (1:50 dilution in water) was placed on top of the samples for 30 minutes. They were then washed in water, and placed in quenching solution (30% hydrogen peroxide diluted in methanol) for 5 minutes. Samples were washed in 1xPBS, then placed in TdT buffer for 5 minutes. The samples were then covered with TdT reaction mix for 1 hour, followed with 1xTdT stop buffer for 5 minutes. Following the wash with 1xPBS, the samples were covered with the antibody solution for 1 hour. They were then washed with 1xPBST and covered with Strep-HRP solution for 10 minutes. The samples were washed with 1xPBS and covered with

TACS Blue Label for 2 minutes. The samples were washed with water and immersed in Nuclear Fast Red for 2 minutes. The samples were then dehydrated and mounted with paraformaldehyde. The nucleus blue and green in color was considered apoptotic. These cells were divided by the number of nucleus present in the sample, as counted by image pro analyzer 6.2.

Lotus Tetragonolobus Lectin (Vector Laboratories)

Lectin binds to the carbohydrate commonly found on PTEC and cuboidal epithelial cells forming part of the Bowman's capsule. It has been shown to be a reliable indicator of an intact glomerulotubular junction as well as PTEC mass (Thornhill et al., 2007). When the ureter is obstructed for two weeks, the cuboidal cells flatten and seal the urinary pole to preserve the Bowman's capsule integrity. This results in an atubular glomerulus (ATG). These glomeruli reduce the amount of filtrate entering the nephrons. In response the PTEC also lose their lectin staining by undergoing atrophy due to the reduced workload and compromised glomerulotubular junction (Forbes et al., 2011). The tubules then degenerate and contribute to fibrosis (Bechtel et al., 2010; Liu, 2012).

Lectin was used to stain for proximal tubular cells. Glomeruli were scored as positive if any staining was present in the capsular area, and lack of any visible staining was scored as a negative glomerulus. This was used to calculate the percentage of stained to the total number of glomeruli. The percentage of unstained glomeruli to the total number of glomeruli was used for atubular calculations.

Samples were first deparaffinized and dehydrated using xylene and 100% ethanol. They were then hydrated in 95%, 70% and water. The samples were washed in water then underwent antigen retrieval in citric acid buffer for 30 minutes. Endogenous peroxidase was applied for 10 minutes followed with washes in PBS. Goat blocking serum was applied for 20 minutes, followed with the application of Lotus Tetragonolobus Lectin Biotin (Vector Laboratories). After washes in 1×TBST, Vectastain ABC solution was applied for 30 minutes. After washes in PBST, ImmPACT DAB (Vector Laboratories) was applied for 1 minute. The slides were observed under a microscope to ensure there was adequate staining. Hemotoxylin was applied followed with washes in water, dehydration and mounting.

3.24 Western blot

The samples were placed in liquid nitrogen until frozen. They were then placed and kept in cryogenic tubes in a liquid nitrogen tank. One sample at a time was removed and extracted to run on a western blot.

The sample was weighed and then added to a cold mortar pestle. This was kept cold by the use of dry ice. After the sample was crushed using a pestle, the powder was placed in an eppendorf tube. These tubes were kept on dry ice until lysis buffer was added. The lysis buffer included 5µg/mL ALLN, along with the components mentioned in section 3.12 . The samples were then sonicated 3 times for 3 seconds with a 2-minute interval in between where they were kept on ice to cool. The samples

were then centrifuged for 10 minutes at 14000 rpm. The protein concentration was detected and then each sample concentration was made to be 1µg/µl and 5xPSB was added. The samples were boiled and kept in -80°C. These samples were then run and the proteins were probed similarly as those in 3.12 of method section.

3.25 IHC Quantification and Statistical Analysis

After taking images from each sample group they were analyzed using Image-pro analyzer 6.2. The stained area/cells were quantified against the total kidney sample area. The percentage was used to compare the different groups. The bar graphs and statistical analysis was assessed using prism 5. The statistical tests performed included T-test, one-way ANOVA and Tukey's honestly significant difference. A P value <0.05 (2-tailed) was considered significant. Data has been presented as mean±SEM.

IV Results

4.1 Aim 1: Does SREBP mediate TNFα-induced apoptosis in tubular cells?

We first established conditions in which TNFα increased the active SREBP-1 levels in HK-2 cells (figure 1a). The levels were found to be elevated after 2 hours of treatment with TNFα (10ng/ml). This significant increase was found sustained at 24 hours of treatment (figure 1b). Active SREBP-2 was found similarly elevated beginning at 6 hours of treatment (figure 2a) and sustained until 24 hours (figure 2b). We then determined whether activated SREBP was functional using a construct containing the SREBP-responsive (SRE) consensus sequence upstream of GFP (figure 3). We used 8 hours of TNFα treatment as this time point provided the most reproducible data. We found a significant increase in SRE promoter activation, confirming that TNFα-induced SREBP activation is transcriptionally functional.

The pathway used by TNFα to induce SREBP cleavage was then evaluated by the use of various inhibitors. These included 4-(2-Aminoethyl) benzenesulfonyl fluoride hydrochloride (AEBSF; Calbiochem, 101500), fatostatin (CHEM Bridge, 5533803) and Akt inhibitor VIII (EMD, 124017). AEBSF is a serine protease inhibitor and thus prevents the cleavage of SREBP to its transcriptionally active form by S1P. The same concentration and treatment time for AEBSF was used as that found in Lhotak et al. (2012). AEBSF at 300μM for 2 hours prior to 2 hour TNFα treatment inhibited the activation of SREBP-1 (figure 4). This suggests that TNFα dependent increase in SREBP-1 activation is dependent upon S1P protease activity.

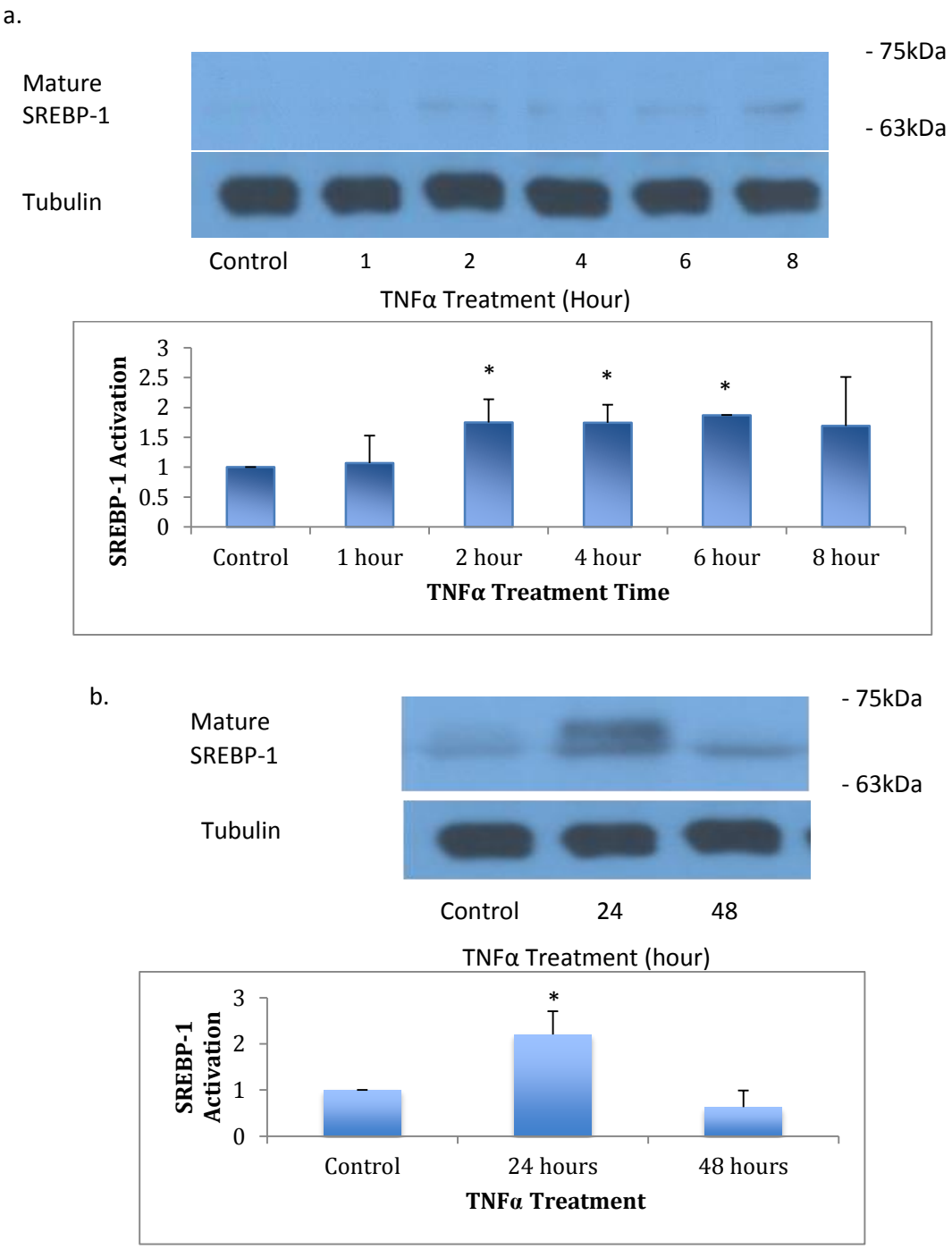

Figure 1: The active SREBP-1 concentration in response to TNFα (10ng/ml) was evaluated in HK-2 cells using densitometric analysis of corresponding western blots. (a)There was a gradual increase in active SREBP-1 levels beginning at 2 hours treatment. (b) Increased active SREBP-1 concentration was maintained at 24hour of treatment. (Mean±SD; *p<0.05; n=3)

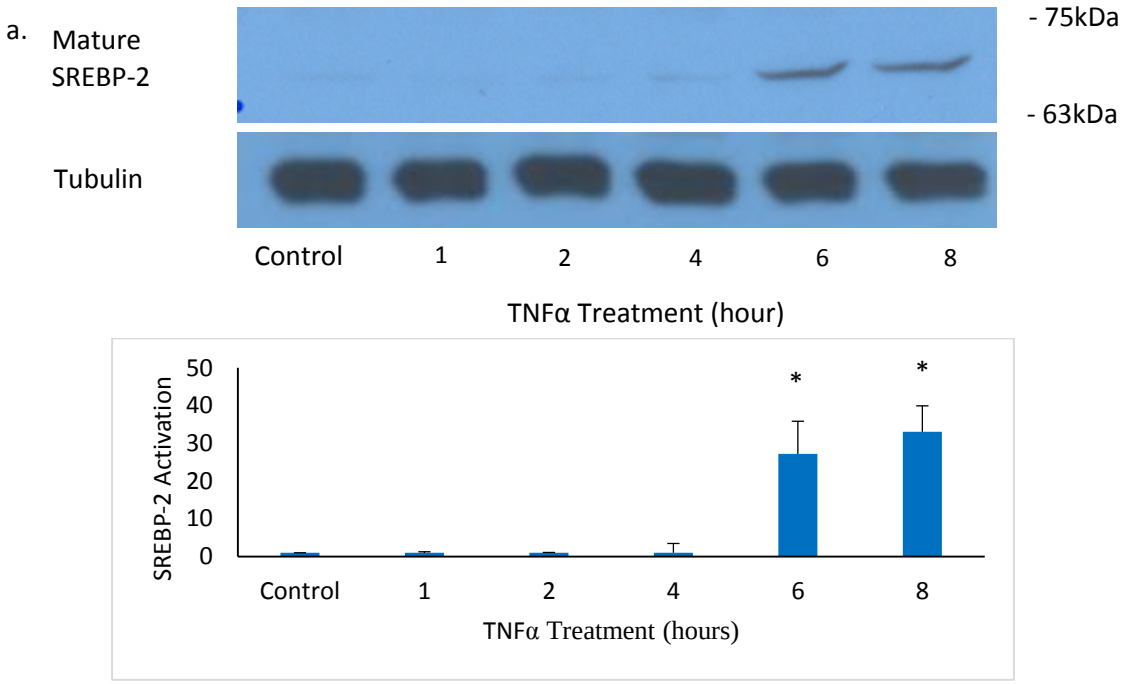

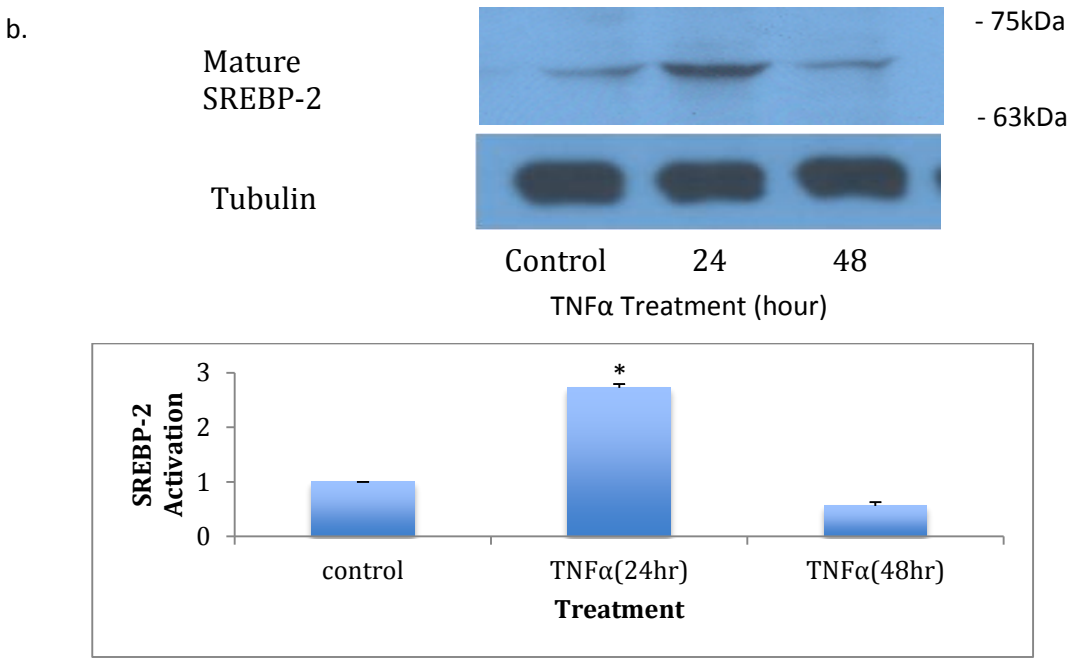

Figure 2: The active SREBP-2 concentration in response to TNFα (10ng/ml) was evaluated in HK-2 cells using densitometric analysis of corresponding western blots. (a) Gradual increase in active SREBP-2 levels beginning at 6 hours of treatment. (b) Increased active SREBP-2 levels were maintained at 24 hours of treatment. (Mean±SEM; n=3; *p<0.05)

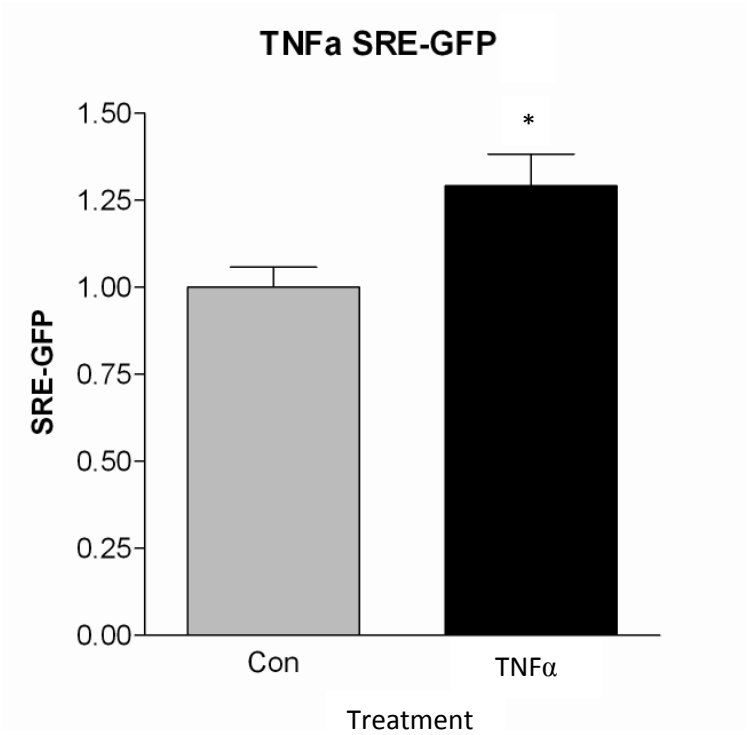

Figure 3: Analysis of SRE-GFP promoter activity at 8 hours of TNFα treatment was evaluated using softmax pro software. There was a significant increase in the GFP levels corresponding to the increased SREBP-1 activation in figure 1 and SREBP-2 levels in figure 2 (mean±SEM; n=8; *$p<0.05$).

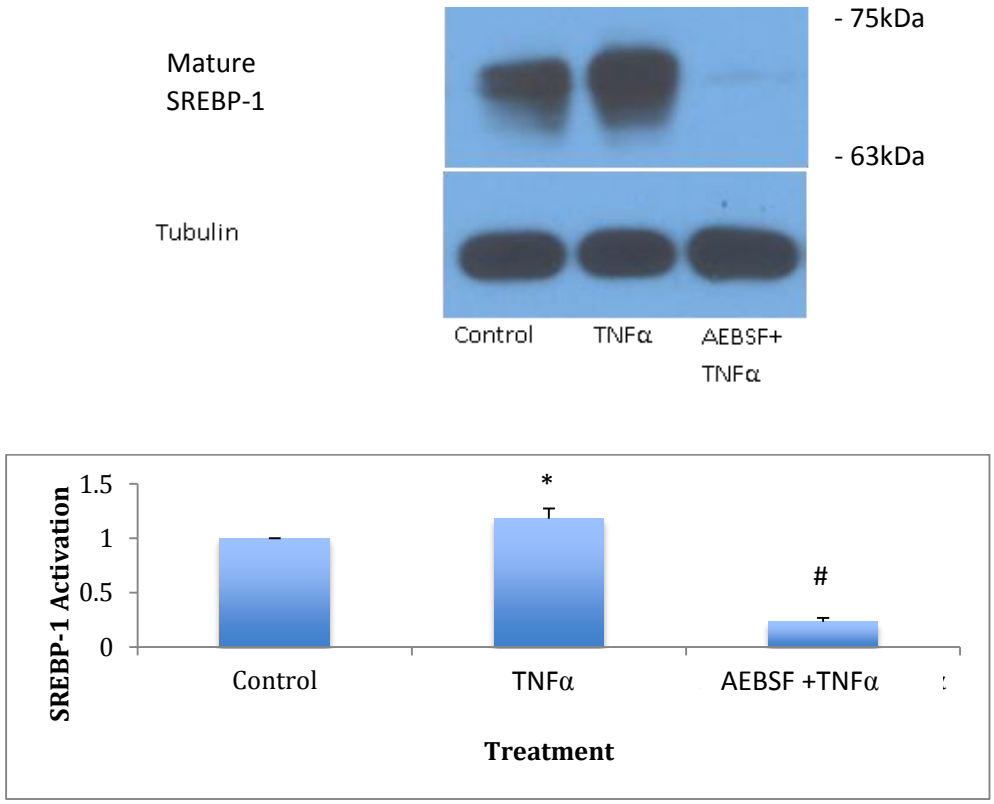

Figure 4: The concentration of active SREBP was found to decrease when the cells were pretreated with AEBSF (300μM) for 1 hour followed with treatment with TNFα (10ng/ml) for 2 hours (mean ± SEM; n=3; *p<0.05 vs. control; #p<0.05 vs. TNFα)

Since AEBSF targets other serine proteases, we used inhibitors that solely target SREBP transport to the Golgi for processing. Fatostatin inhibits the translocation of SREBP from ER to Golgi by binding to SCAP. The concentration and time interval used for fatostatin was as that used for kidney glomerular mesangial cells in Uttarwar et al. (2012). Fatostatin pretreatment for 4 hours (figure 5a) and 2 hours (figure 5b) at a concentration of 20μM, followed with TNFα treatment for 2 hours, inhibited the activation of SREBP-1. Unfortunately SREBP-2 is found to be activated at 6 hours, and could not be evaluated in these experiments.

We also decided to investigate the role of Akt, as it has similarly been found to be involved in the anterograde transport of SREBP from ER to Golgi (Du et al., 2006). We treated HK-2 cells with time intervals of TNFα treatment. By utilizing the pAkt antibody, we were able to detect activated Akt. There was an increased phosphorylation of Akt in a time dependent manner of TNFα treatment (figure 6a). The Akt inhibitor VIII was confirmed to reduce the level of pAkt (figure 6b) and downregulate the activation of SREBP-1 (figure 6c).

Using these inhibitors, we thus determined that SCAP-mediated transport to the Golgi for processing regulates TNFα-induced SREBP-1 activation. Furthermore, Akt signaling is also required for SREBP-1 activation.

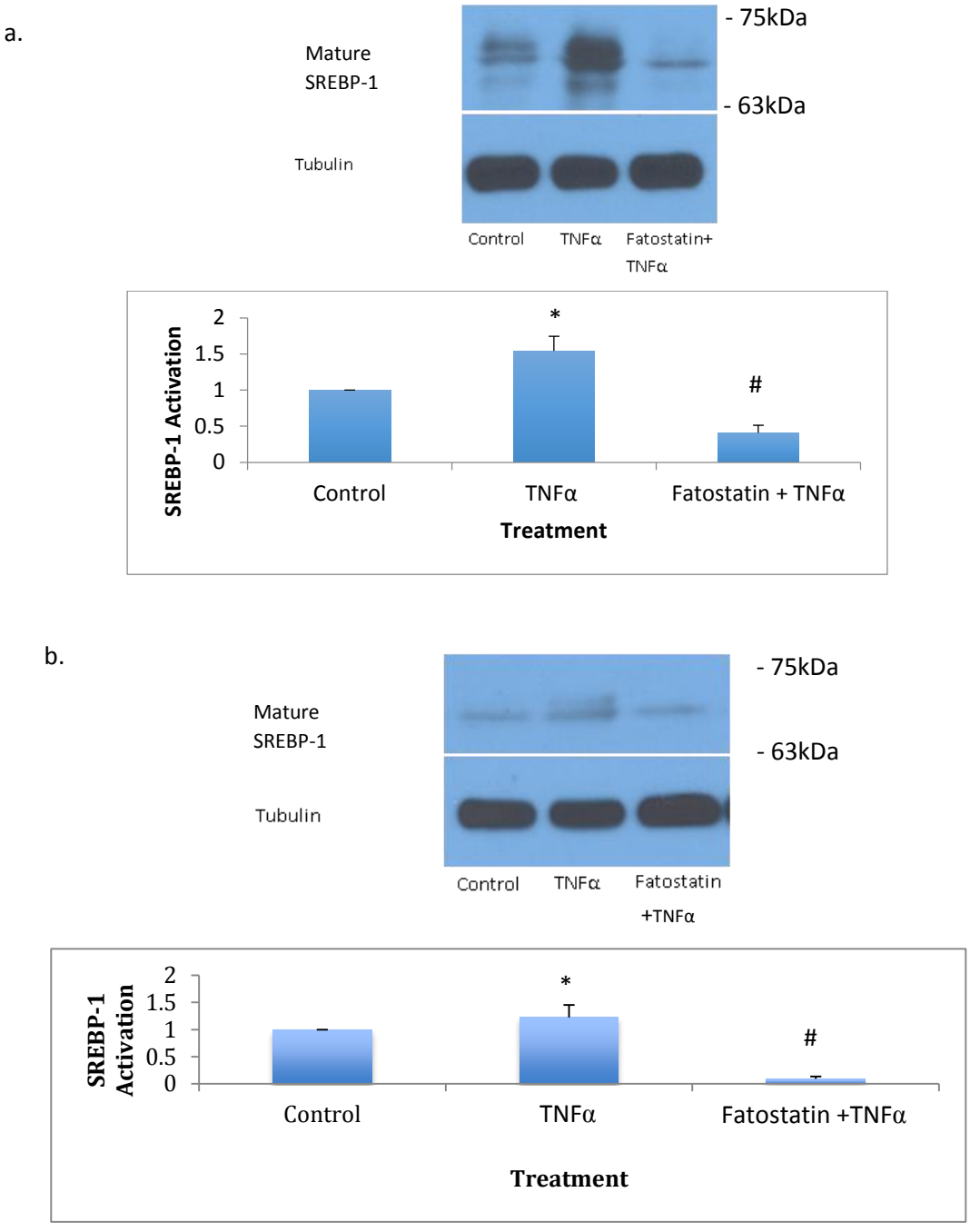

Figure 5: The active SREBP-1 concentration in response to TNFα (10ng/ml) and fatostatin (20μM) treatment was evaluated in HK-2 cells using densitometric analysis of corresponding western blots. (a) Following a 4 hour pretreatment of fatostatin, there was a significant decrease in the concentration of active SREBP-1. (b) Similar impediment was observed after 2 hours of pretreatement of fatostatin. (Mean±SEM; n=3; *p<0.05 vs. control; #p<0.05 vs. TNFα)

a.

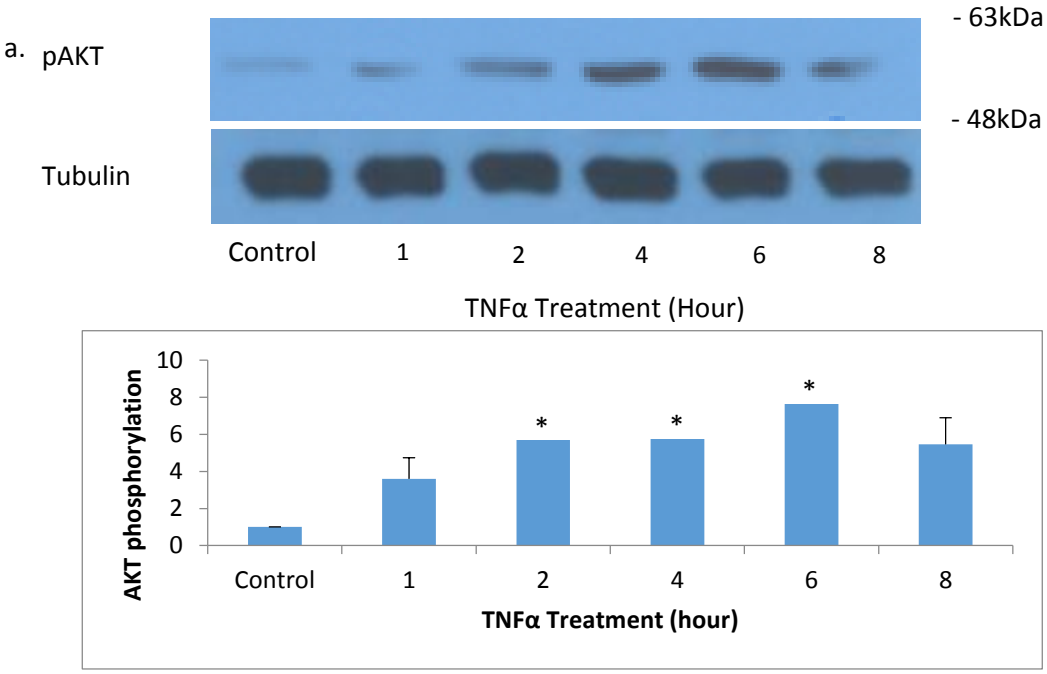
pAKT
Tubulin
- 63kDa
- 48kDa
Control
1
2
4
6
8
TNFα Treatment (Hour)
AKT phosphorylation
10
8
6
4
2
0
*
*
*
Control
1
2
4
6
8
TNFα Treatment (hour)

b.

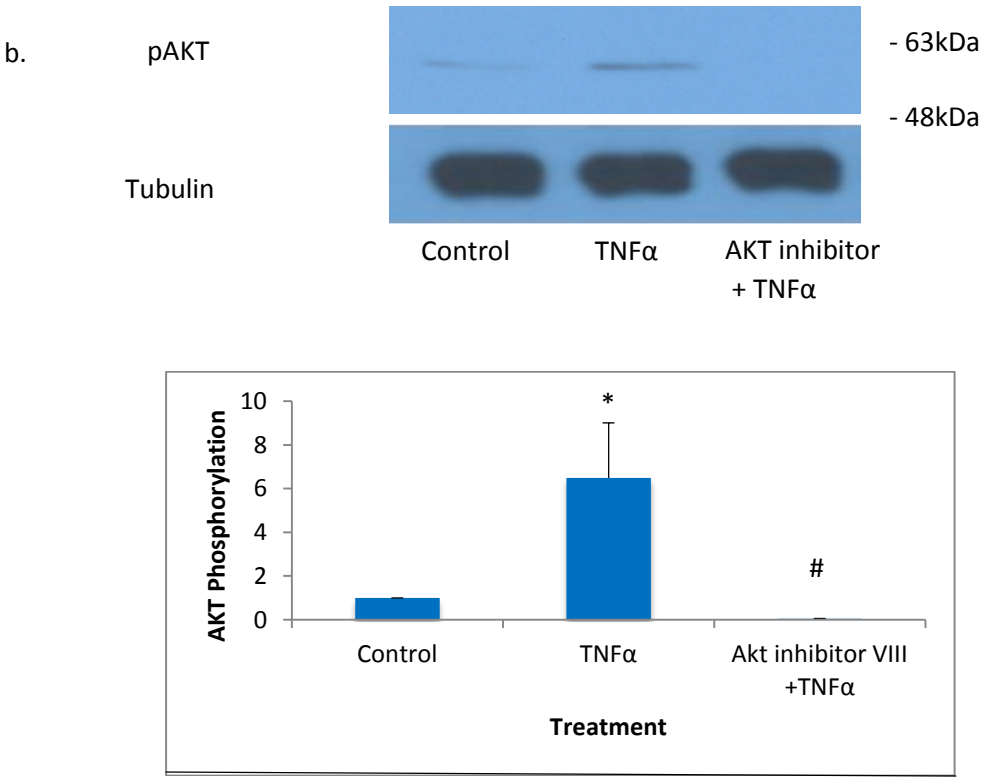
pAKT
Tubulin
- 63kDa
- 48kDa
Control
TNFα
AKT inhibitor + TNFα
AKT Phosphorylation
10
8
6
4
2
0
*
#
Control
TNFα
Akt inhibitor VIII +TNFα
Treatment

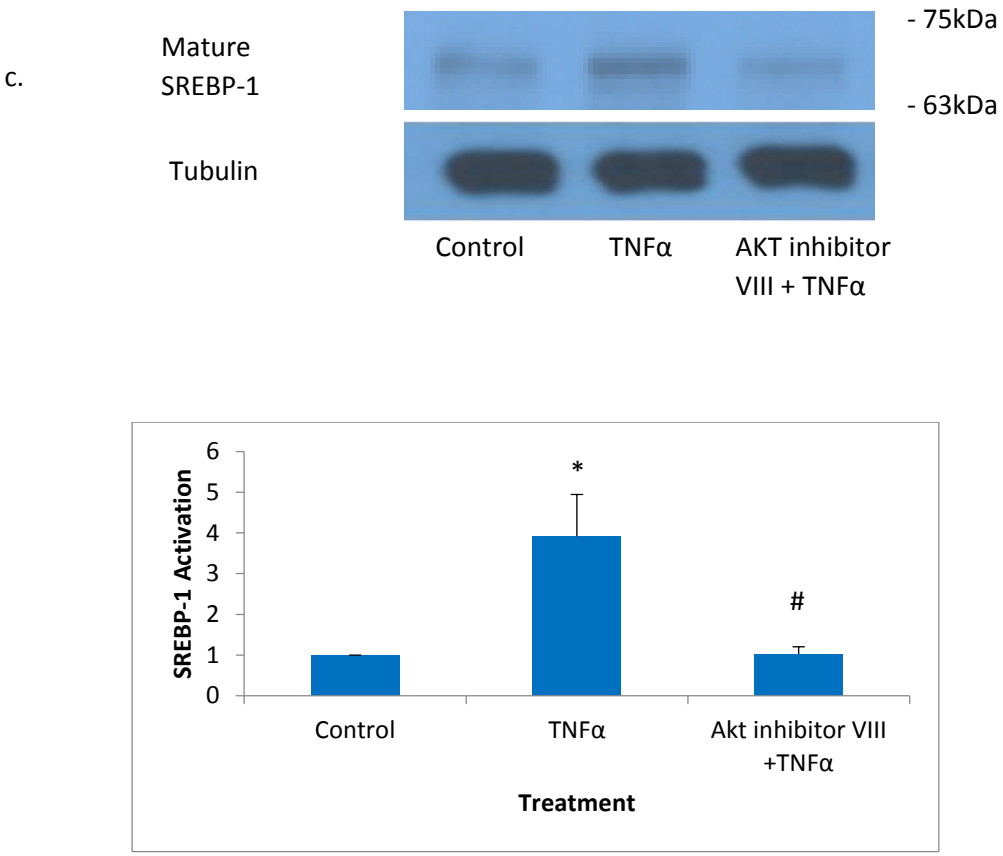

Figure 6: The active SREBP-1 concentration and pAkt in response to TNFα (10ng/ml) and 10μM of Akt inhibitor VIII treatment was evaluated in HK-2 cells using densitometric analysis of corresponding western blots. (a) There was a gradual increase of activated Akt levels beginning at 2 hours of treatment (b) Akt inhibitor was found to inhibit active Akt expression when cells were treated with the inhibitor for 1 hour followed with TNFα for 2 hours. (c) With the same treatment as (b), there was a decrease in the concentration of active SREBP-1 (mean±SEM; n=3; *$p<0.05$ vs. Con; #$p<0.05$ vs. TNFα).

We next evaluated the Caspase-3 contribution to this pathway as it has been linked to intrinsic and extrinsic mediated apoptosis (Elmore, 2007; Thornberry and Lazebnik, 1998). Various studies have found caspase-3 activated indirectly by caspase 8 in TNFα-induced apoptosis (Wang et al., 2008). HK-2 cells treated with TNFα were found to have increased cleavage of caspase-3 in a time-dependent manner starting at 2 hours of treatment (figure 7a). The cleavage of caspase-3 was still significantly increased at 24 hours after TNFα treatment (figure 7b). This suggests that caspase-3 activation in HK-2 cells mediates apoptosis. When this expression increases, the probability of the cell undergoing apoptosis increases.

We then evaluated whether caspase-3 activation was upstream or downstream of SREBP activation. Caspase-3 cleavage by TNFα treatment remained unchanged when fatostatin was applied (figure 8). This suggests that caspase-3 may not lie downstream of SREBP activation.

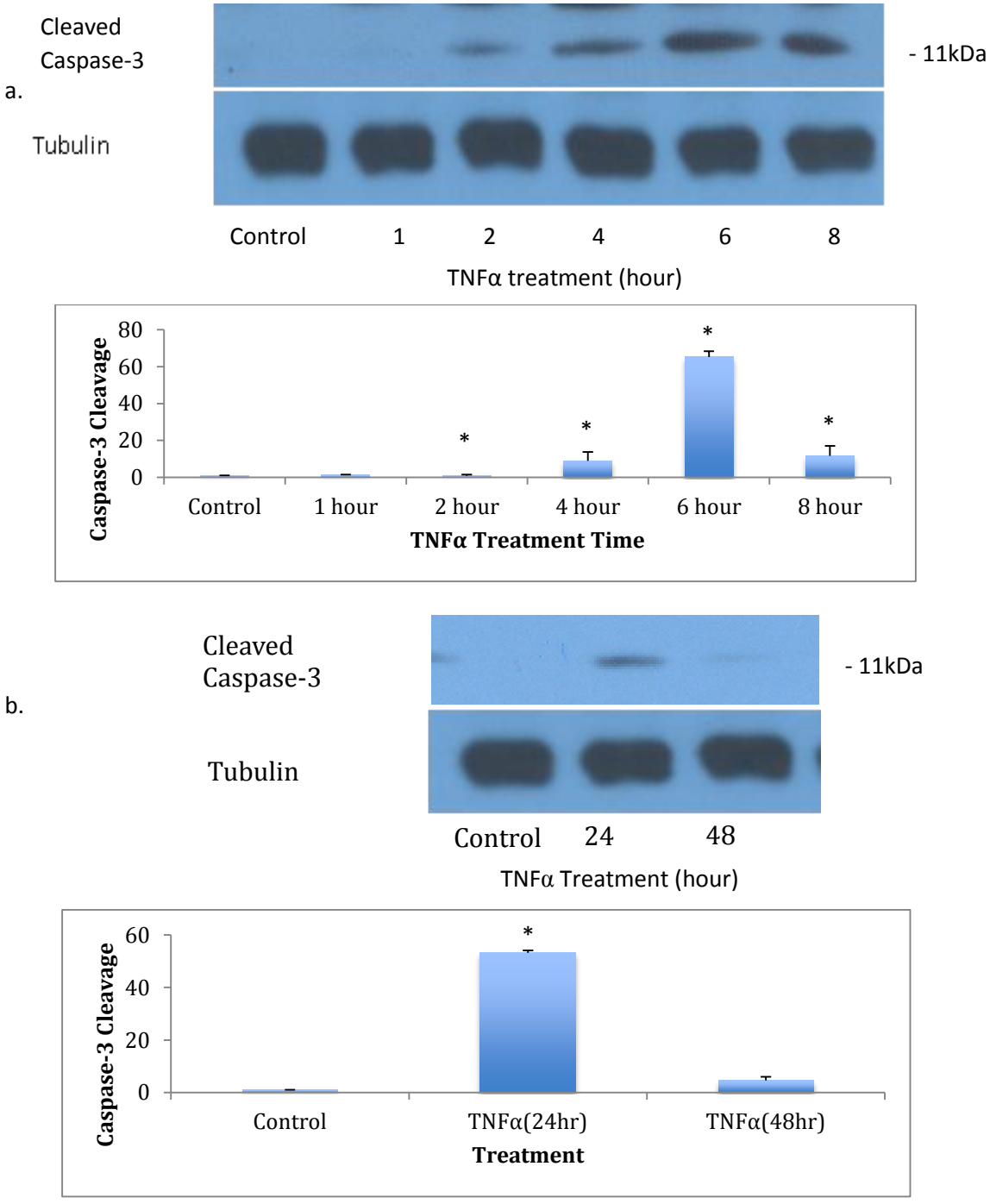

Figure 7: The active Caspase-3 cleavage in response to TNFα (10ng/ml) treatment was evaluated in HK-2 cells using densitometric analysis of corresponding western blots (a) The caspase-3 cleavage was found to be upregulated at 2 hours of TNFα treatment. (b) This increase was maintained at 24hours of treatment. (Mean±SEM; n=3; *p<0.05 vs. control; #p<0.05 vs. TNFα)

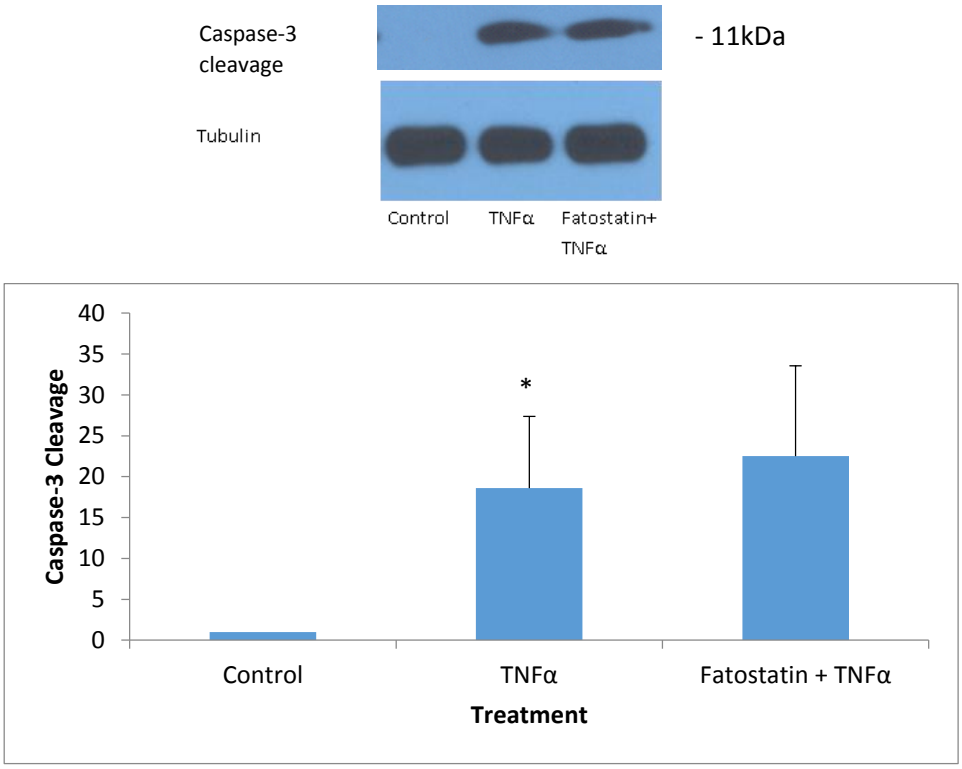

Figure 8: The active Caspase-3 cleavage in response to TNFα (10ng/ml) and fatostatin (20μM) treatment was evaluated in HK-2 cells using densitometric analysis of corresponding western blots. (Mean±SEM; n=3; *p<0.05 vs. con)

We then assessed whether or other caspases lie upstream of TNFα-mediated SREBP cleavage. The specific inhibitors used were benzyloxycarbonyl-Val-Ala-Asp fluoromethyl ketone (zVAD; Cederlane, FMK001) and caspase-3 inhibitor VIII (EMD, 219013). The broad caspase inhibitor, zVAD, binds to the catalytic site of caspase protease to prevent apoptosis induction. The concentration of the broad caspase inhibitor, zVAD, used for these experiments, is the same as that found in Boise and Thompson, (1997). One hour pretreatment with 50μM of ZVAD decreased SREBP-1 activation after 2 hours of TNFα treatment (data not shown). Similarly, when cells were pretreated for 1 hour of zVAD, followed by 6 hours of treatment with TNFα, caspase-3 and SREBP-1 activation were decreased significantly (figure 9).

The second inhibitor we used was the specific caspase-3 inhibitor. This inhibitor binds to an allosteric site of caspase-3 to inhibit the cleavage of Poly (ADP-ribose) polymerase (PARP). PARP is a polymerase found downstream of caspase-3 which assists in the pro-survival pathway. PARP normally uses NAD^+ and ATP to repair the DNA breakage (Ame et al., 1999; Schreiber et al., 2002). When there is a large amount of DNA breakage, as found during apoptosis, PARP is inactivated via caspase-3 cleavage at a conserved sequence. This is done so the cell can preserve the amount of readily available energy (Kaufmann et al., 1993). If this enzyme is not inactivated, the cell can undergo caspase independent cell death, which can result in inflammatory injury (Hong et al., 2004; Yu et al., 2002). Therefore, cleavage of PARP is necessary during apoptosis.

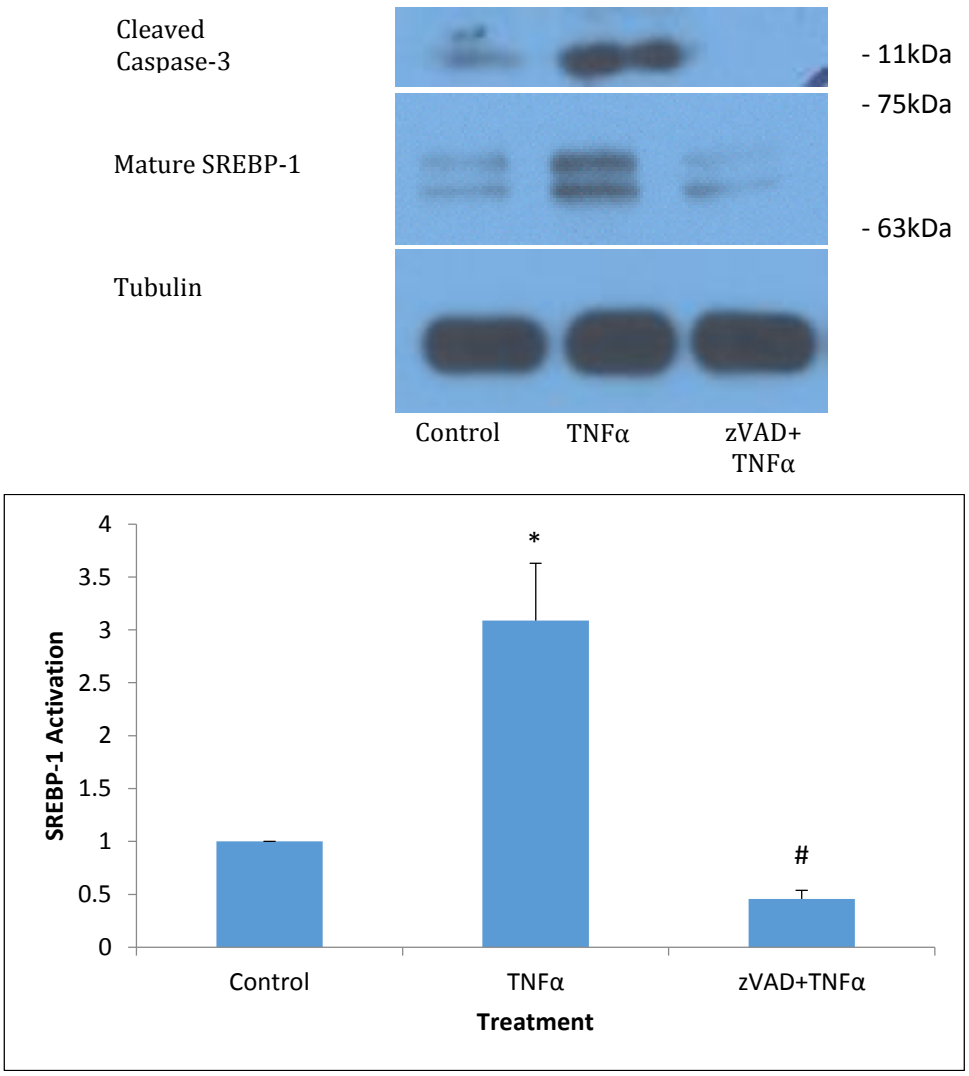

Figure 9: TNFα (10ng/ml) treatment for 2 hours, followed with pretreatment of zVAD (50μM), resulted in a decreased activation of SREBP-1. (Mean±SEM; n=3; *p<0.05 vs. control; #p<0.05 vs. TNFα)

Figure 10 illustrates the gradual increase of PARP cleavage in a time dependent manner of TNFα treatment. We found PARP cleavage to be decreased in the presence of zVAD (figure 11). This is the result of an inhibition of Caspase-3. Since zVAD is a broad caspase inhibitor, we assessed the importance of caspase-3 by using its specific inhibitor. PARP is cleaved at Asp214 and Gly215 at the DEVD site to generate 85kDa and 24kDa fragments (Kaufmann et al., 1993; Nicholson et al., 1995). The caspase-3 inhibitor VIII (EMD) inhibits the active DEVD site in a reversible substrate competitive manner to prevent the cleavage of PARP. This means the caspase found upstream as well as the cleavage of caspase-3 will be unaffected by this inhibitor. In our studies, the use of 10μM of caspase-3 inhibitor resulted in a decrease in SREBP-1 activation (figure 12).

We also assessed the caspase-3 and PARP response to fatostatin treatment. Both of these enzymes were found to be unaffected by this inhibitor. In aggregate, this data suggests that caspase-3 lies upstream of TNFα induced SREBP activation, and is cleaving SREBP in a non-SCAP mediated pathway. This is also supported by the findings of Higgins and Ionone (2001), which shows SREBP cleavage by caspase 3.

With these experiments we have come to understand the potential pathway that TNFα may use to cleave and activate SREBP. It seems that this transcription factor may be activated in a SCAP and non-SCAP mediated pathway. We decided to use the fatostatin drug, to investigate the effects SCAP mediated inhibition of SREBP cleavage for our aim 2.

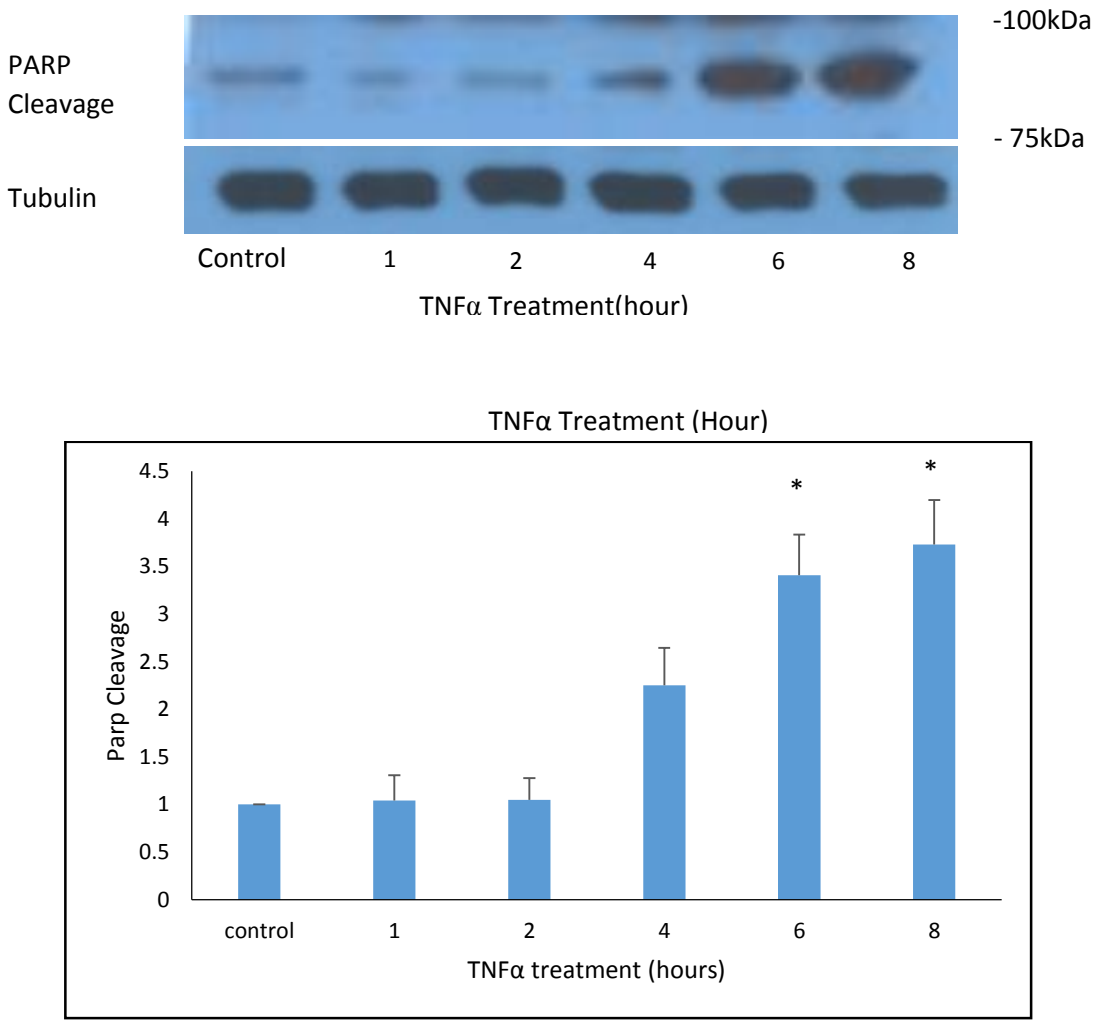

Figure 10: There was a time dependent increase of PARP cleavage, beginning at 6 hours of TNFα (10ng/ml) treatment evaluated using densitometric analysis corresponding to its western blot. (Mean±SEM; n=3; *p<0.04 vs. control)

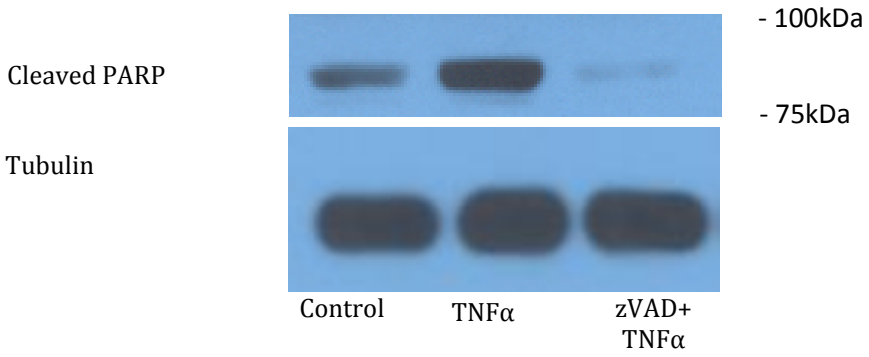

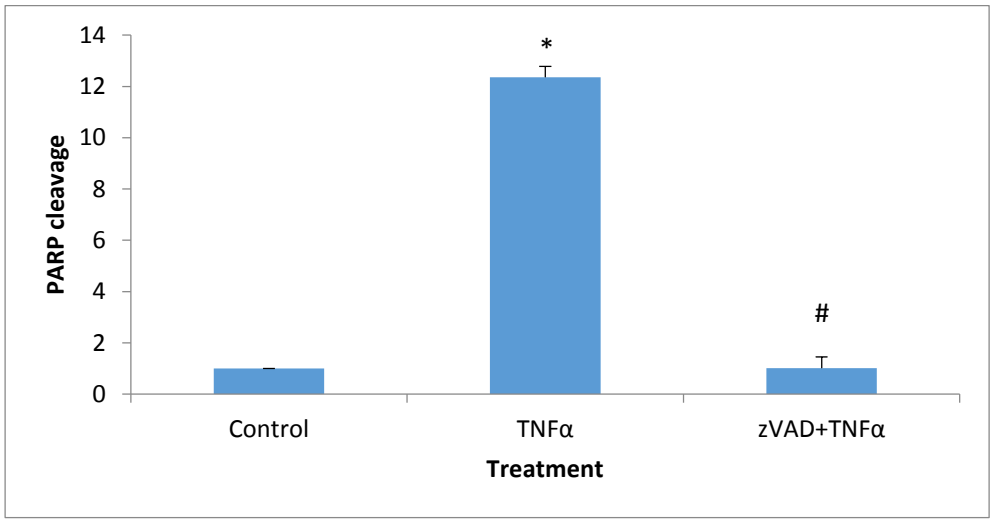

Figure 11: Decreased cleavage of PARP in HK-2 cells in response to pretreatment of zVAD (50μM) for 1 hour and TNFα (10ng/ml) treatment for 6 hours evaluated with densitometric analysis corresponding to its western blot. (Mean±SEM; n=3; *p<0.05 vs. control; #p<0.05 vs. TNFα)

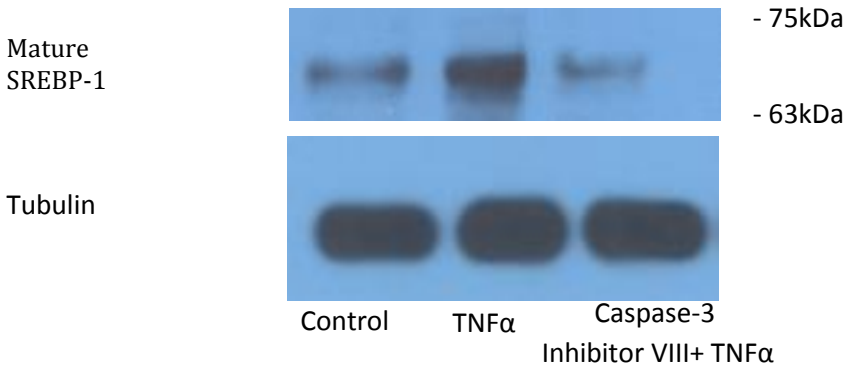

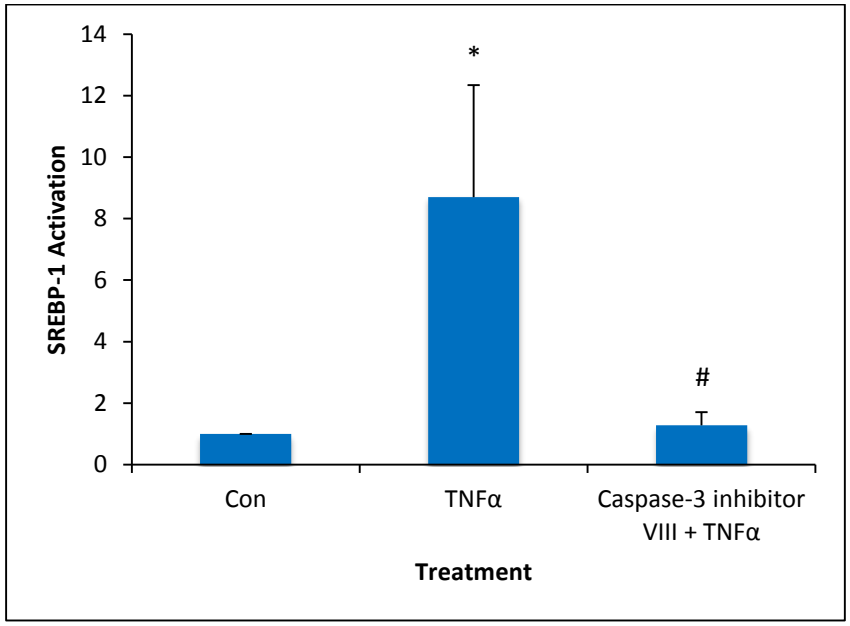

Figure 12: The activated SREBP-1 was found to be significantly reduced when TNFα (10ng/ml) was treated for 2 hours followed with caspase-3 inhibitor VIII (10μM) treatment for 1 hour evaluated using densitometric analysis corresponding it its western blot. (Mean±SEM; n=3; *p<0.05 vs. Control; #p<0.05 vs. TNF).

4.2 Aim 2: Does SREBP inhibition attenuate apoptosis and fibrosis in vivo in the UUO model?

Since SREBP is activated by TNFα, which is a major mediator of tubular cell apoptosis and renal fibrosis in the UUO model (Misseri et al., 2004; Misseri et al., 2005), we investigated if SREBP inhibition would alter the pathology in this model. We decided to use the SCAP inhibitor fatostatin given its specificity for inhibiting SREBP and its prior in vivo use in mice (Kamisuki et al., 2009).

We first confirmed that SREBP was activated in the UUO model. Although the expression of SREBP-1 (figure 13a-d) and SREBP-2 (figure 14a-d) were found to be higher at different days after UUO, apoptosis is known to reach maximum levels at day 14 (Kennedy et al., 1994; Chevalier, 1996). We thus decided to use 14-day of UUO to compare the effects of fatostatin.

We first assessed kidneys weight in the two UUO groups. The kidneys were weighed following the removal of the surrounding fascia. Figure 15 illustrates that although there is a decrease in the average kidney weight in the UUO+Fato group compared to the UUO group, no significant difference was found.

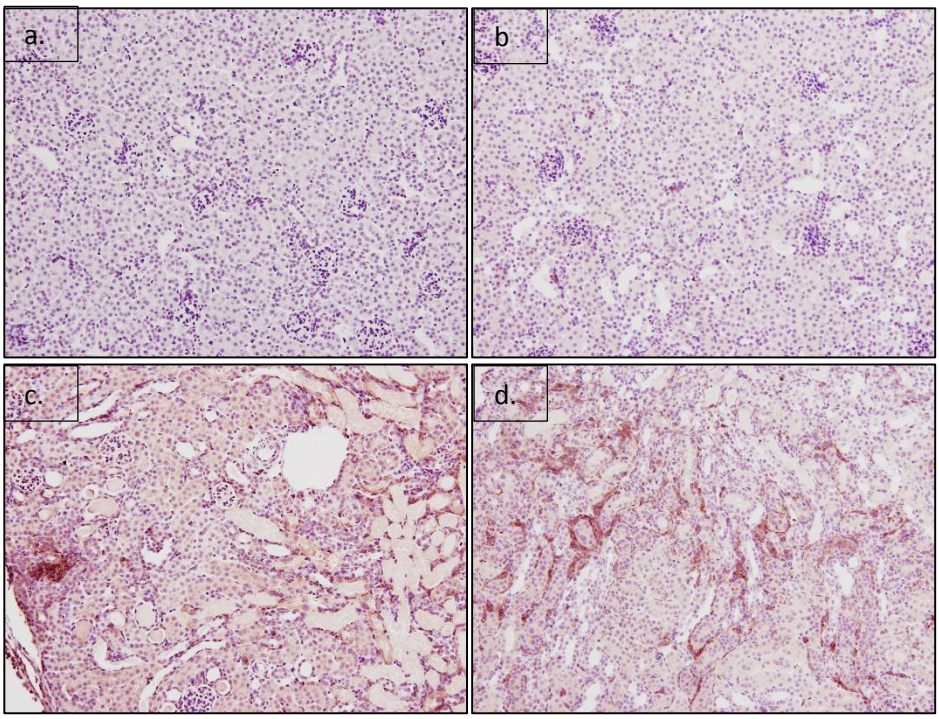

Figure 13: SREBP-1 expression for (a) control, (b) 1 day UUO, (c) 3 day UUO, and (d) 7 day UUO.

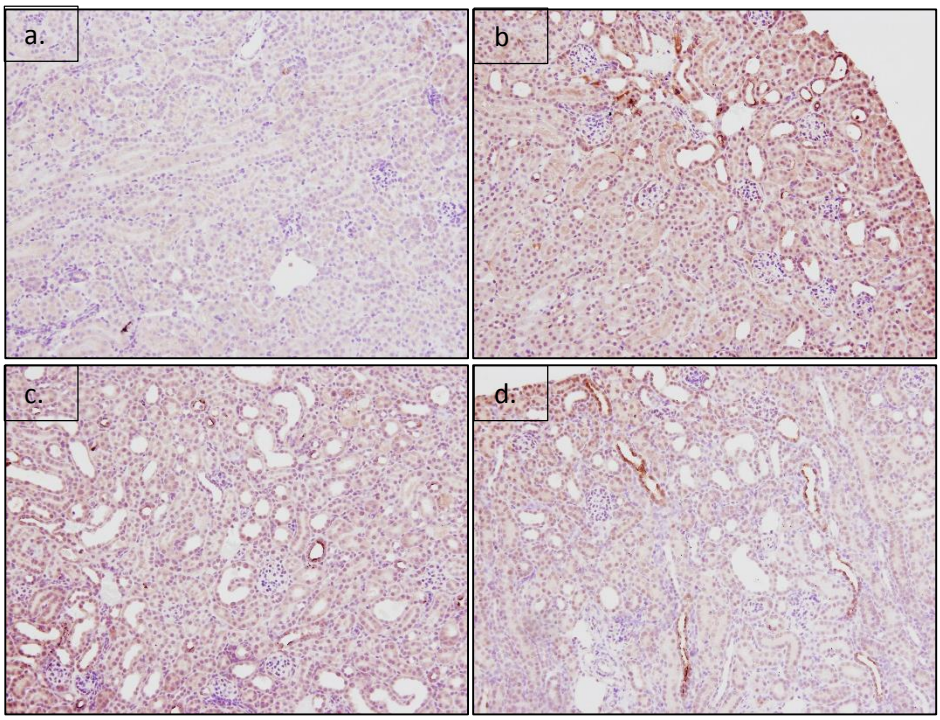

Figure 14: SREBP-2 expression for (a) control, (b) 1 day UUO, (c) 3 day UUO, and (d) 7 day UUO.

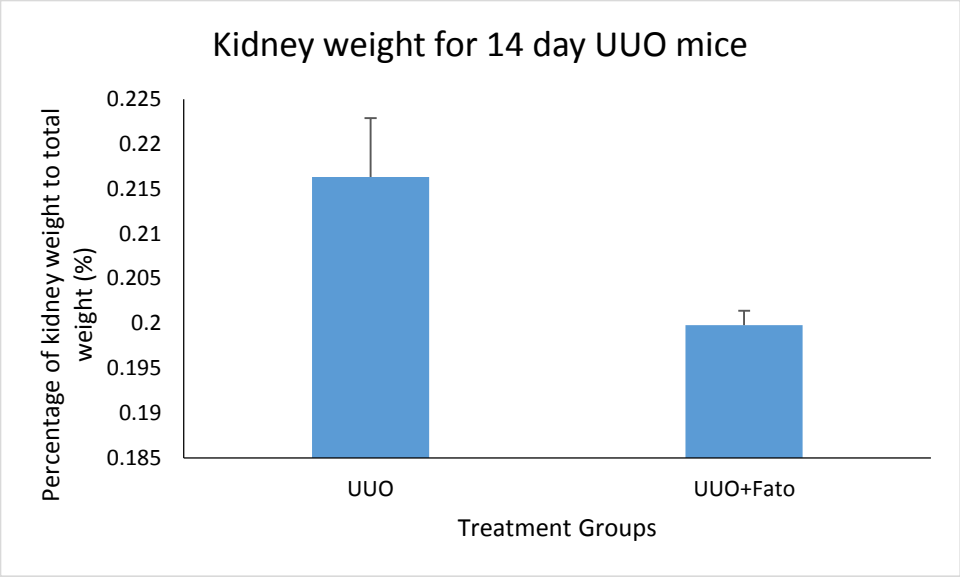

Figure 15: The percentage of kidney weight to body weight was evaluated in the UUO groups. Although the average weight for UUO group was higher than UUO-fatostatin group, there was no significance (mean±SEM; n=5 UUO; n=7 UUO+fato).

We then evaluated the amount of SREBP-1 activation by western blots (figure 16a). Fatostatin reduced activated SREBP-1 at 7 days after UUO compared to the saline-treated UUO group. Similar results were found when IHC was used for the kidney samples (figure 16b). Since fatostatin also inhibits SREBP-2, we evaluated its activation. We found similar results, with SREBP-2 activation significantly down-regulated by fatostatin after 7 days as assessed by western blot (figure 17a). We also found a substantial decrease in the SREBP-2 using IHC (figure 17b). This indicates that fatostatin is effective in vivo in inhibiting SREBP activation. Additional mice will be needed for results to reach statistical significance.

I then stained for apoptosis using the TUNEL kit. For the IHC slides the number of green and blue nuclei were counted and compared to the total number of nuclei counted by the image-pro analyzer 6.2. The UUO-fatostatin group was found to have reduced TUNEL staining compared to the UUO group ($p < 0.05$; figure 18e), suggesting that fatostatin treatment reduced tubular cell apoptosis. The corresponding pictures for the TUNEL staining are found in figure 18a-d.

a.

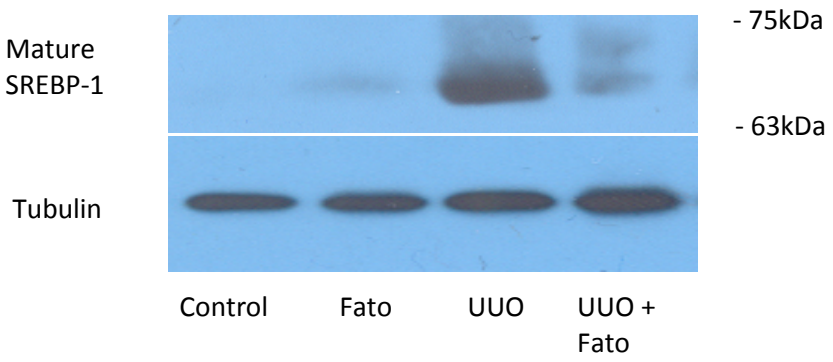
Mature
SREBP-1
Tubulin
- 75kDa
- 63kDa
Control
Fato
UUO
UUO +
Fato

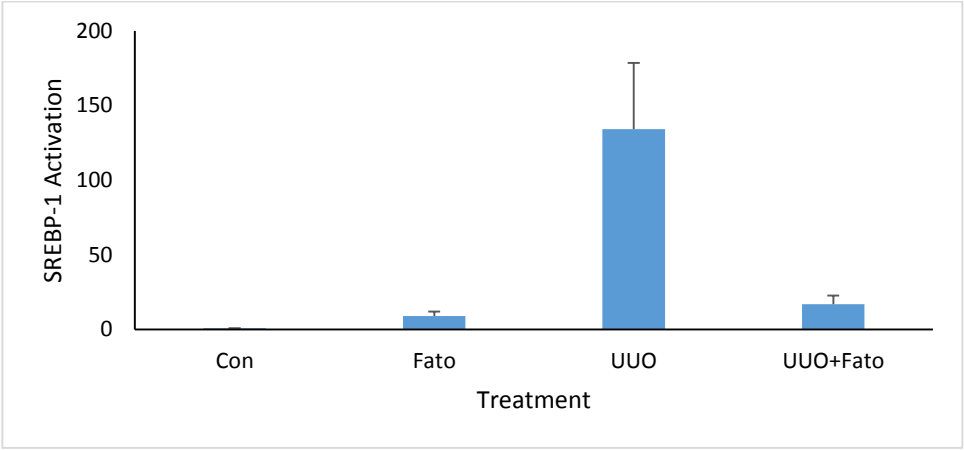
SREBP-1 Activation
200
150
100
50
0
Con
Fato
UUO
UUO+Fato
Treatment

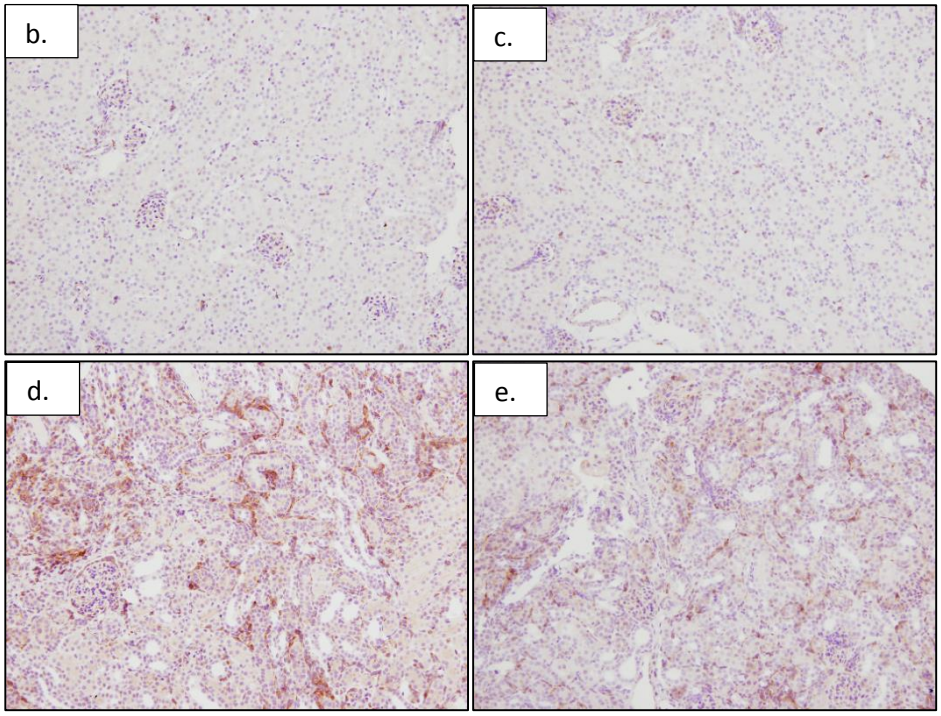

Figure 16: SREBP-1 levels were evaluated using western blots and IHC for 7 day UUO groups and their corresponding controls. (a) Western blot and corresponding densitometric graph showing reduced activated SREBP-1 protein levels in the UUO-fatostatin group compared to UUO group. (Mean±SEM; n=3 per group). IHC slides showing a decreased expression of SREBP-1 in the UUO-fatostatin group compared to UUO. (b) Control. (c) Fatostatin. (d) UUO. (e) UUO-Fatostatin.

a.

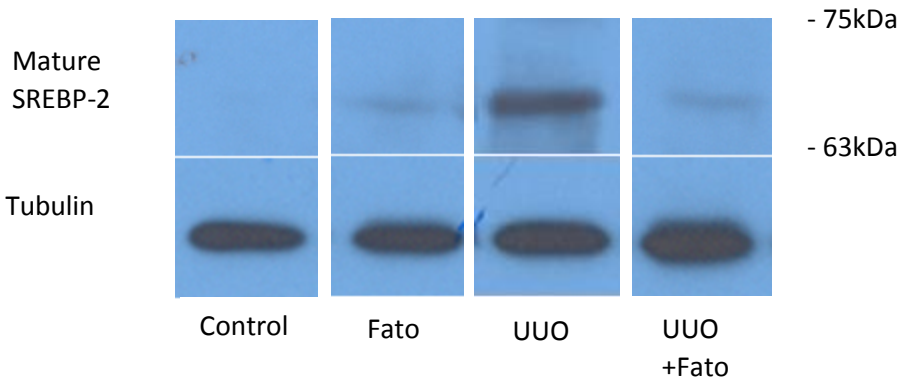
Mature
SREBP-2
Tubulin
- 75kDa
- 63kDa
Control
Fato
UUO
UUO
+Fato

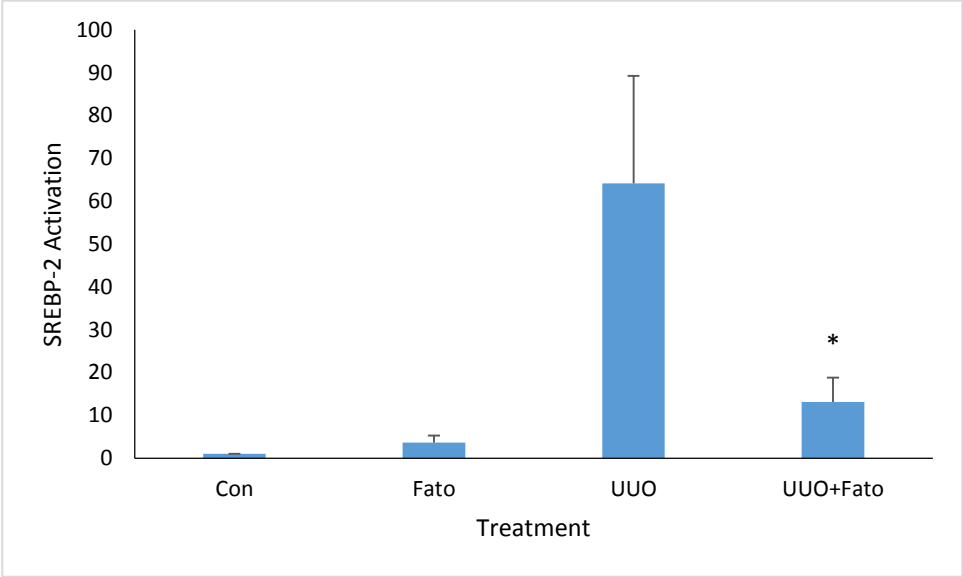
SREBP-2 Activation
100
90
80
70
60
50
40
30
20
10
0
*
Con
Fato
UUO
UUO+Fato
Treatment

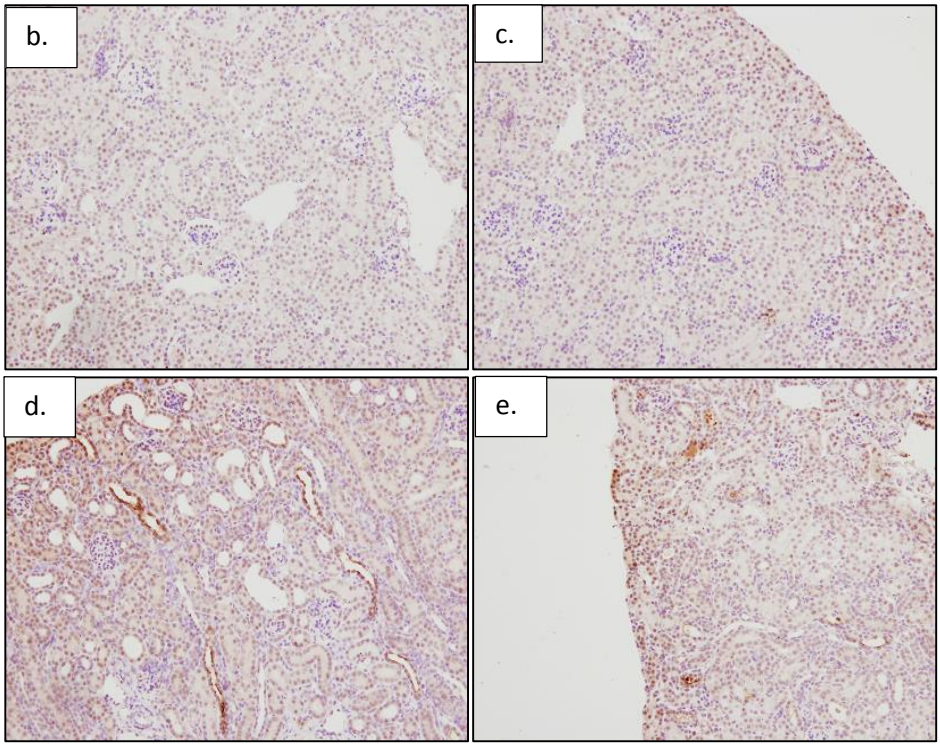

Figure 17: SREBP-2 levels were evaluated using western blots and IHC for 7 day and 14 day UUO mice. (a) Western blot and its corresponding densitometric analysis showing a reduced SREBP-2 activation in the 7 day UUO-fatostatin group compared to UUO group (mean±SEM; *$p<0.05$ vs. UUO; n=3 per group). IHC slides showing a decreased expression of SREBP-2 in UUO-fatostatin group compared to UUO. (b) Control. (c) Fatostatin. (d) UUO. (e) UUO-Fatostatin.

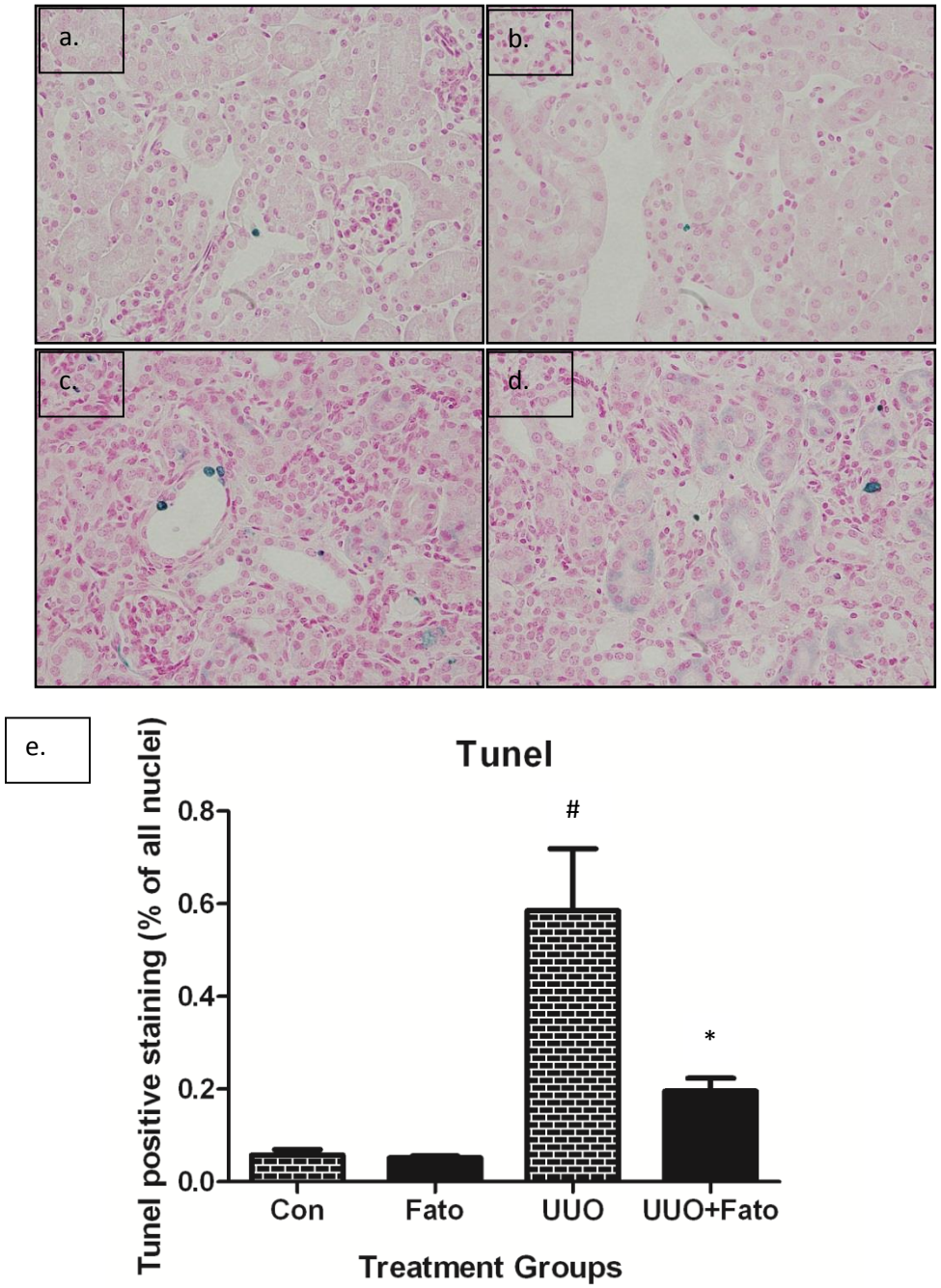

Figure18: The amount of apoptosis was evaluated in the cortex region of kidney samples for control (a). (b) Fatostatin. (c) UUO. (d) UUO with fatostatin treatment. (e) The percentage of apoptotic cells to the total number of cells were evaluated in the 14 day UUO animals and their respective controls. (Mean±SEM; #$p<0.001$ vs. Con;*$p<0.05$ vs. UUO)

I next evaluated the proximal tubular mass and glomerular tubular junction integrity by staining for lectin. The amount of proximal tubule staining was higher in the UUO-fatostatin group compared to the UUO group (Figure 19e; $p<0.05$). The corresponding pictures for the proximal tubule staining are found in figure 19 a-d. This shows some preservation of proximal tubular cell mass.

We then investigated the effects of fatostatin on integrity of the glomerulotubular junction in the UUO model. We compared the amount of positive glomeruli (lectin stained) to the total amount of glomeruli in the section. Figure 20e shows that there was a higher percentage of positive glomerular staining in the UUO-fatostatin group compared to the UUO group ($p<0.05$). The percentage of atubular glomeruli (the glomeruli that have lost their staining) to the total number of glomeruli was an inverse of figure 20e (figure 20f). This shows that fatostatin is protective against the loss of glomerulotubular integrity and suggests that fatostatin thereby preserves the number of functional glomeruli. The corresponding pictures can be found in figure 20a-d.

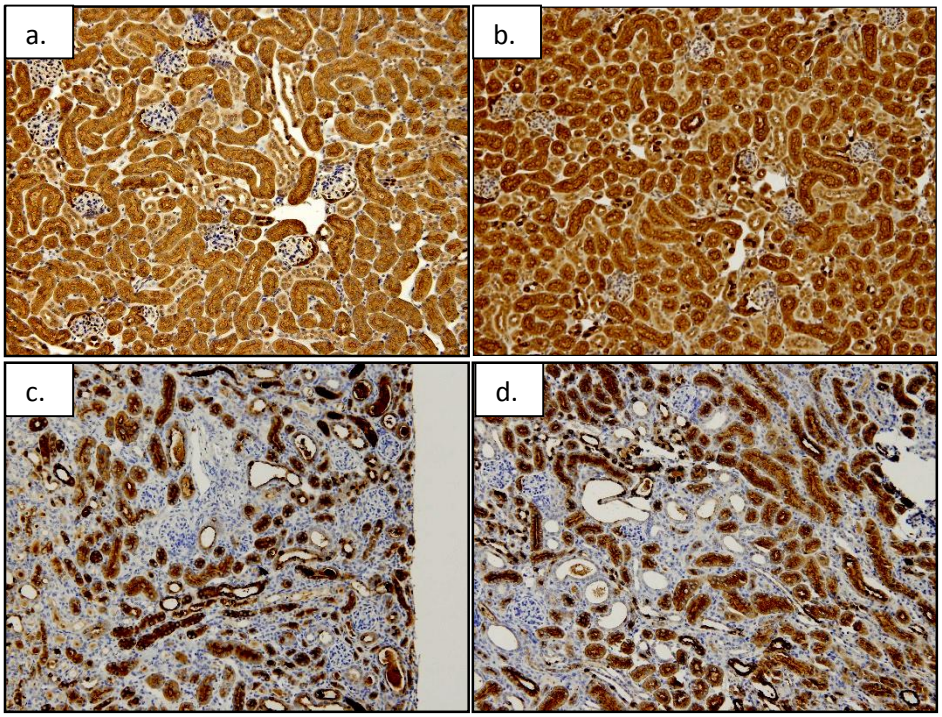

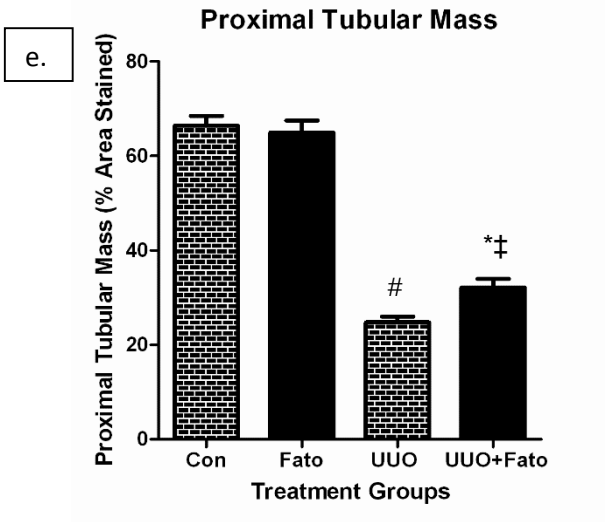

Figure 19: The amount of lectin staining was evaluated in the cortex region of kidney samples for Control (a). (b) Fatostatin. (c) UUO. (d) UUO with fatostatin treatment. (e) The percentage of positive glomeruli stained compared to the total number of glomeruli was evaluated in the 14day UUO mice and their respective controls. (Mean ±SEM; #p<0.0001 vs. Control; ‡p<0.0001 vs. Fatostatin; *p<0.001 vs. UUO; n=3 for controls; n=7 for UUO groups).

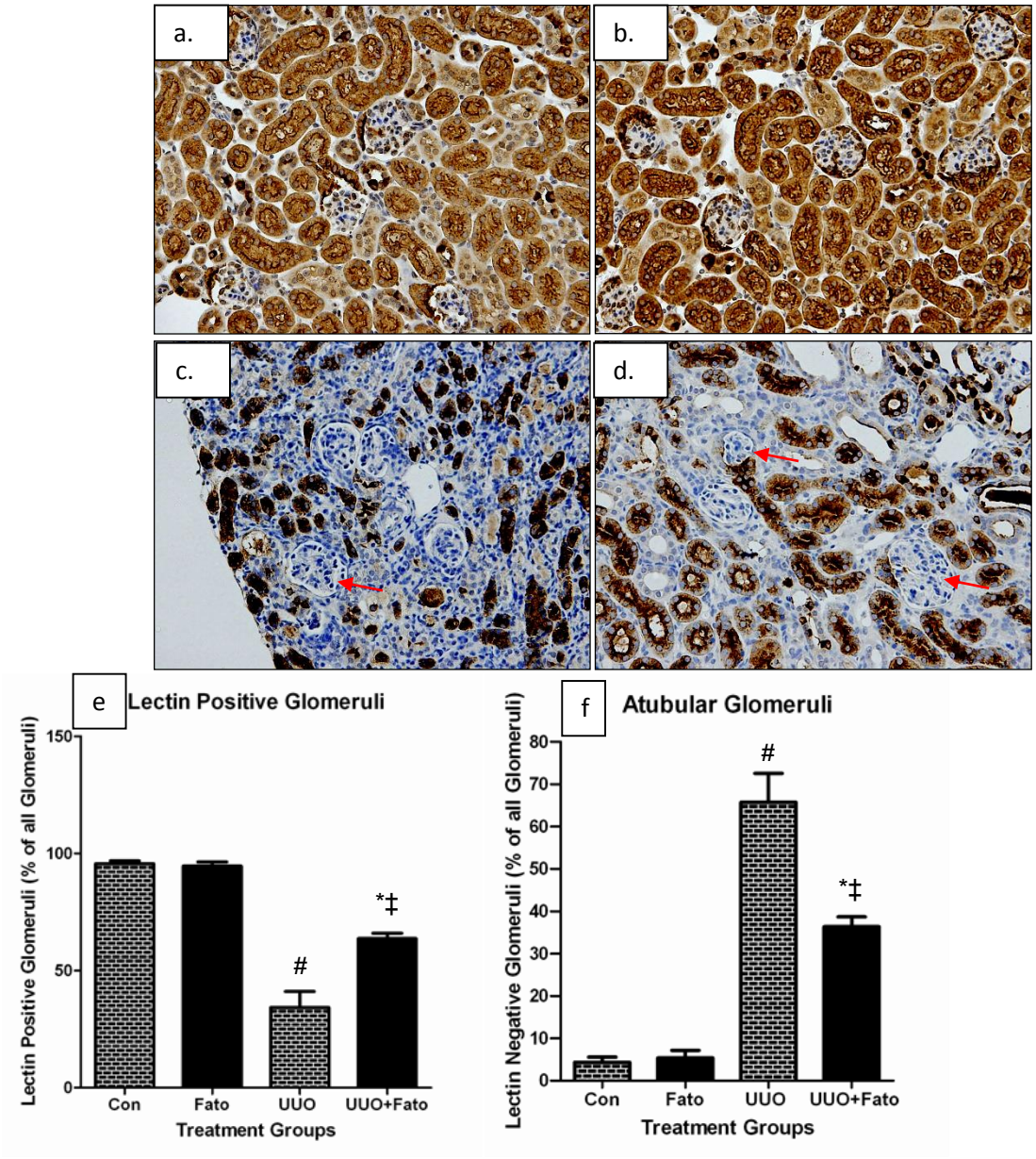

Figure 20: Glomerulotubular integrity indicated by Lotus staining. (a) Control. (b) Fatostatin. (c) UUO. (d) UUO with fatostatin treatment. (e) The percentage of positive glomeruli stained compared to the total number of glomeruli was evaluated in the 14day UUO mice and their respective controls. (Mean ±SEM; #p<0.0001 vs. Control; ‡p<0.05 vs. Fatostatin; *p<0.0001 vs. UUO; n=3 for controls; n=7 for UUO groups). The percentage of unstained glomeruli to the total number of glomeruli was evaluated in the 14day UUO mice and their respective controls (means ±SEM; #p<0.0001 vs. Control; ‡p<0.001 vs. Fatostatin; *p<0.05 vs. UUO; n=3 for controls; n=7 for UUO groups; arrows showing the positive glomeruli).

We next evaluated the degree of fibrosis present in each group by investigating collagen and fibronectin deposition. The first stain we performed on each group was the Masson Trichrome stain. Using this stain, we found that fatostatin attenuated fibrosis after UUO (figure 21e, $p<0.05$). The corresponding pictures can be found in figure 21 a-d.

We next evaluated specific collagen and fibronectin staining. We did this to assess the specific matrix proteins upregulated in this model. We investigated collagen I and III by using the PSR kit (figure 22e). The UUO group had more PSR stain compared to the UUO-fatostatin group ($p<0.05$). The corresponding pictures can be found in figure 22a-d. Fibronectin deposition was also found to be similarly significantly higher in the UUO group compared to the UUO-fatostatin group (figure 23e; $p<0.05$). The corresponding pictures can be found in figure 23 a-d.

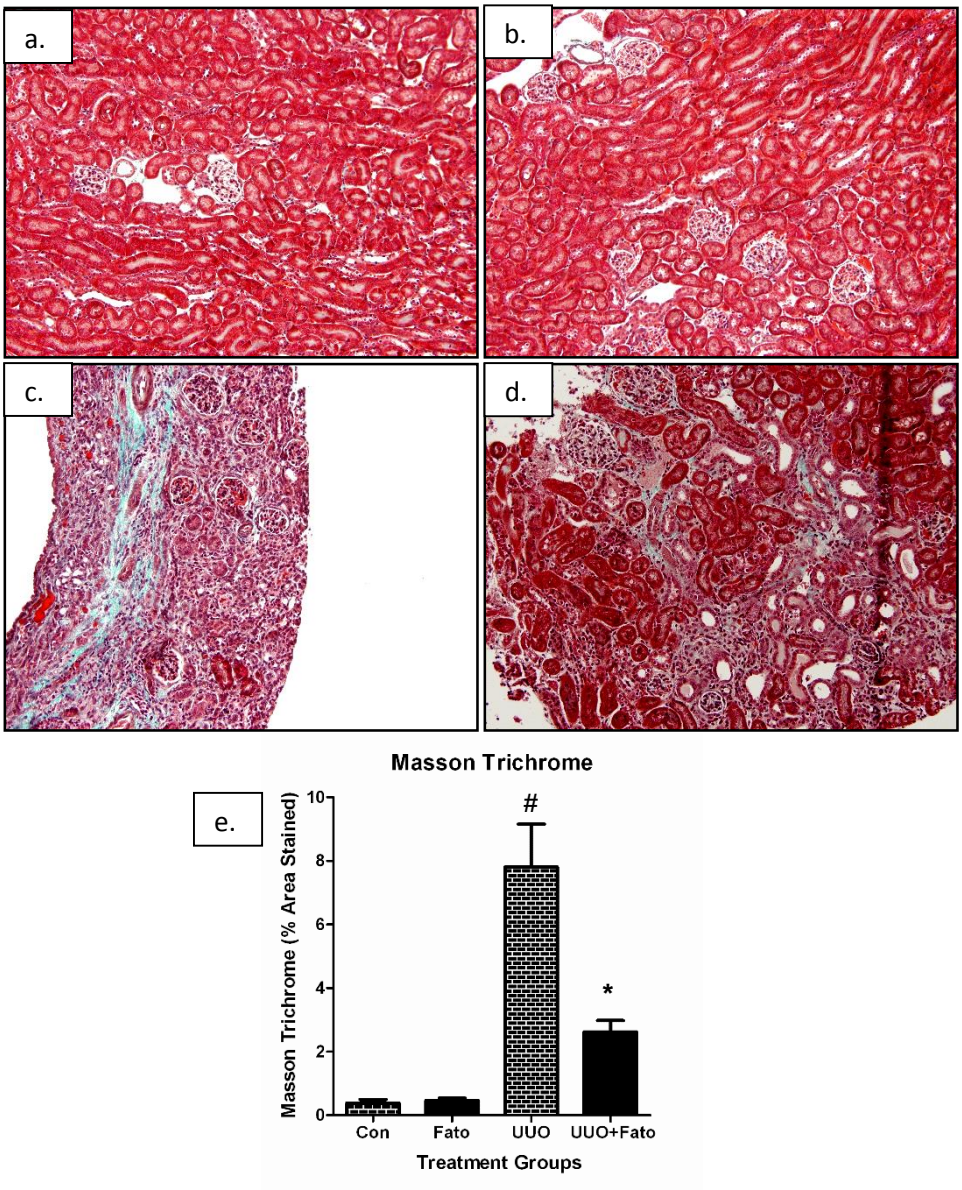

Figure 21: The amount of collagen deposition was evaluated using Masson Trichrome staining (a) Control. (b) Fatostatin. (c) UUO with saline treatment. (d) UUO with fatostatin treatment. (e) The percentage of connective tissue staining to the total area of tissue was evaluated in the 14day UUO mice and their respective controls. (Mean ±SEM; #$p<0.0001$ vs. Control; *$p<0.0001$ vs. UUO; n=3 for controls; n=7 for UUO groups)

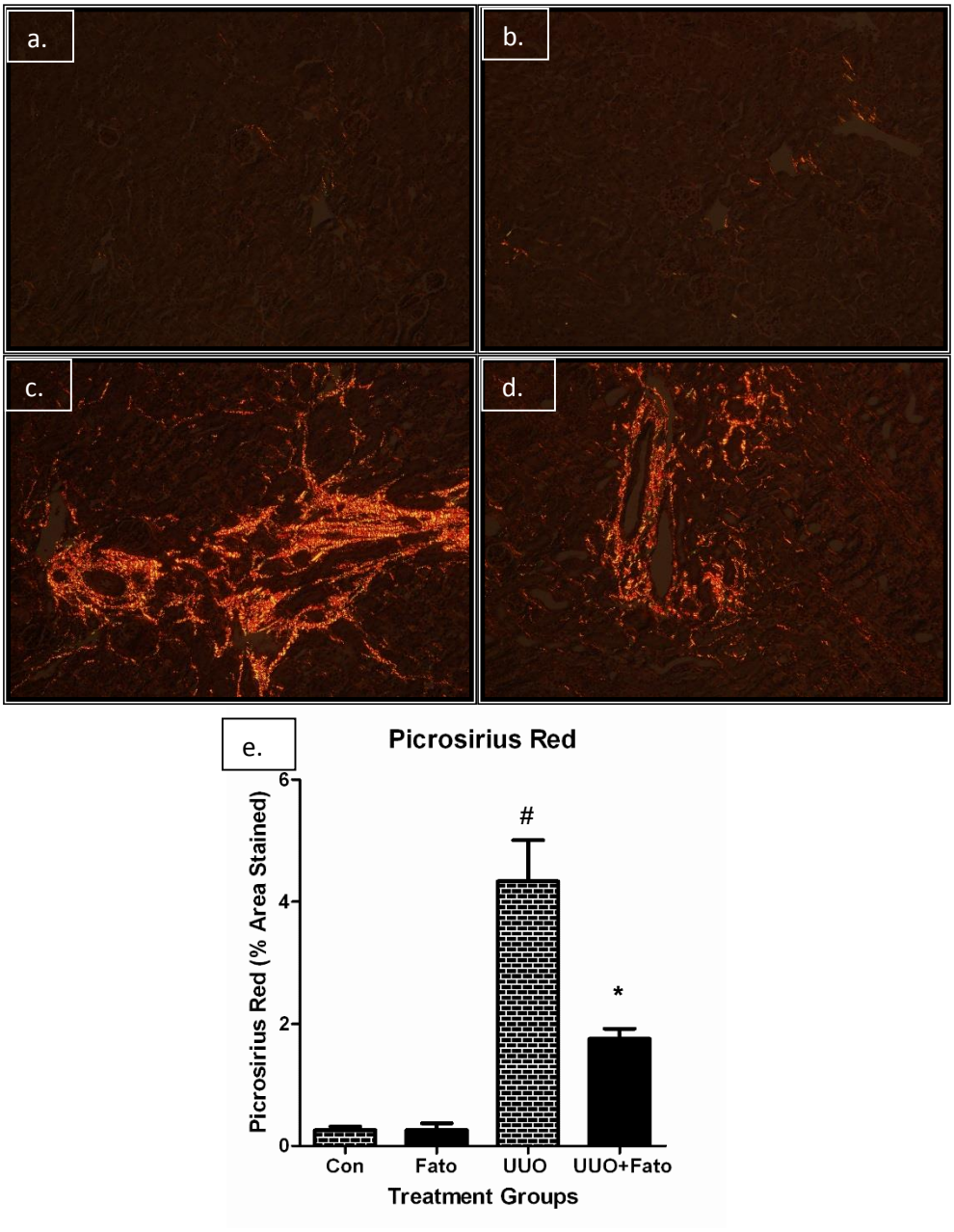

Figure 22: The amount of collagen I and III deposition was evaluated using PSR kit and polarized light. (a) Control. (b) Fatostatin. (c) UUO. (d) UUO with fatostatin treatment. (e) The percentage of collagen I and III staining to the total area of tissue was evaluated in the 14day UUO mice and their respective controls. (Mean ±SEM; #p<0.0001 vs. Control; *p<0.0001 vs. UUO; n=3 for controls; n=7 for UUO groups).

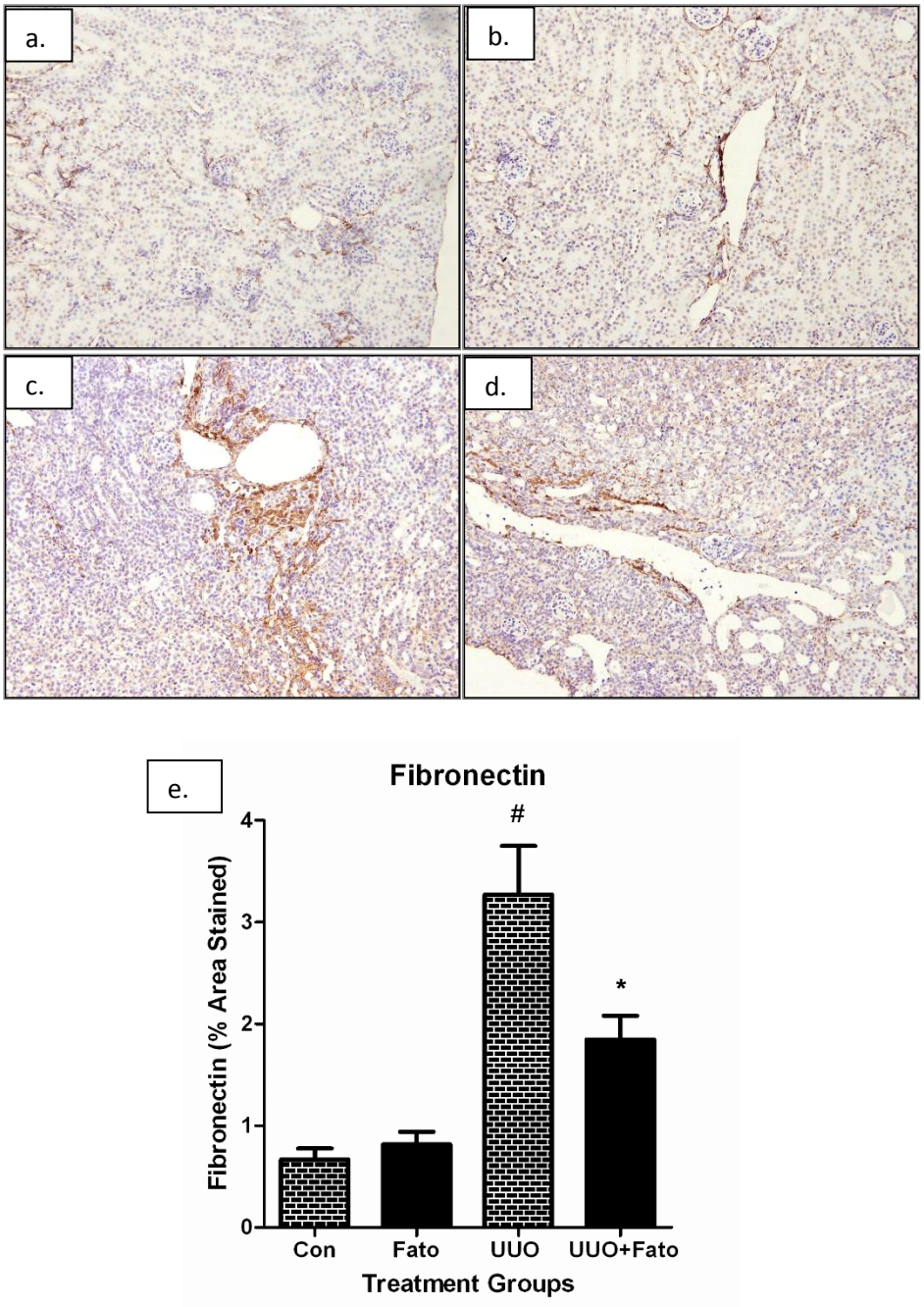

Figure 23: The amount of fibronectin expression was evaluated. (a) Control. (b) Fatostatin. (c) UUO. (d) UUO with fatostatin treatment. (e) The percentage of fibronectin staining to the total area of tissue was evaluated in the 14day UUO mice and their respective controls. (Mean ±SEM; #p<0.0001 vs. Control; *p<0.05 vs. UUO; n=3 for controls; n=7 for UUO groups).

We next assessed well-described contributors to the fibrotic response in this model. We first assessed the extent of myofibroblast presence, a cell type which actively contributes to fibrosis through deposition of collagen, fibronectin and other matrix proteins (Lin et al., 2008). Myofibroblasts are marked by their expression of αSMA, and this was used to identify them in sections (figure 24a-d). The UUO-fatostatin group was found to have less αSMA staining compared to the UUO group (figure 24e; $p<0.05$).

We then investigated the number of inflammatory cells present in each kidney section. T cells have been thought to contribute to initiation and progression of renal fibrosis through fibrocyte activation increasing the amount of ECM deposition (Niedermeier et al., 2009). T cell infiltration was evaluated using an antibody targeting CD3 expression, a T-cell antigen (figure 25a-d). The infiltration was found to be less in the UUO-fatostatin group compared to the UUO group (figure 25e; $p<0.05$).

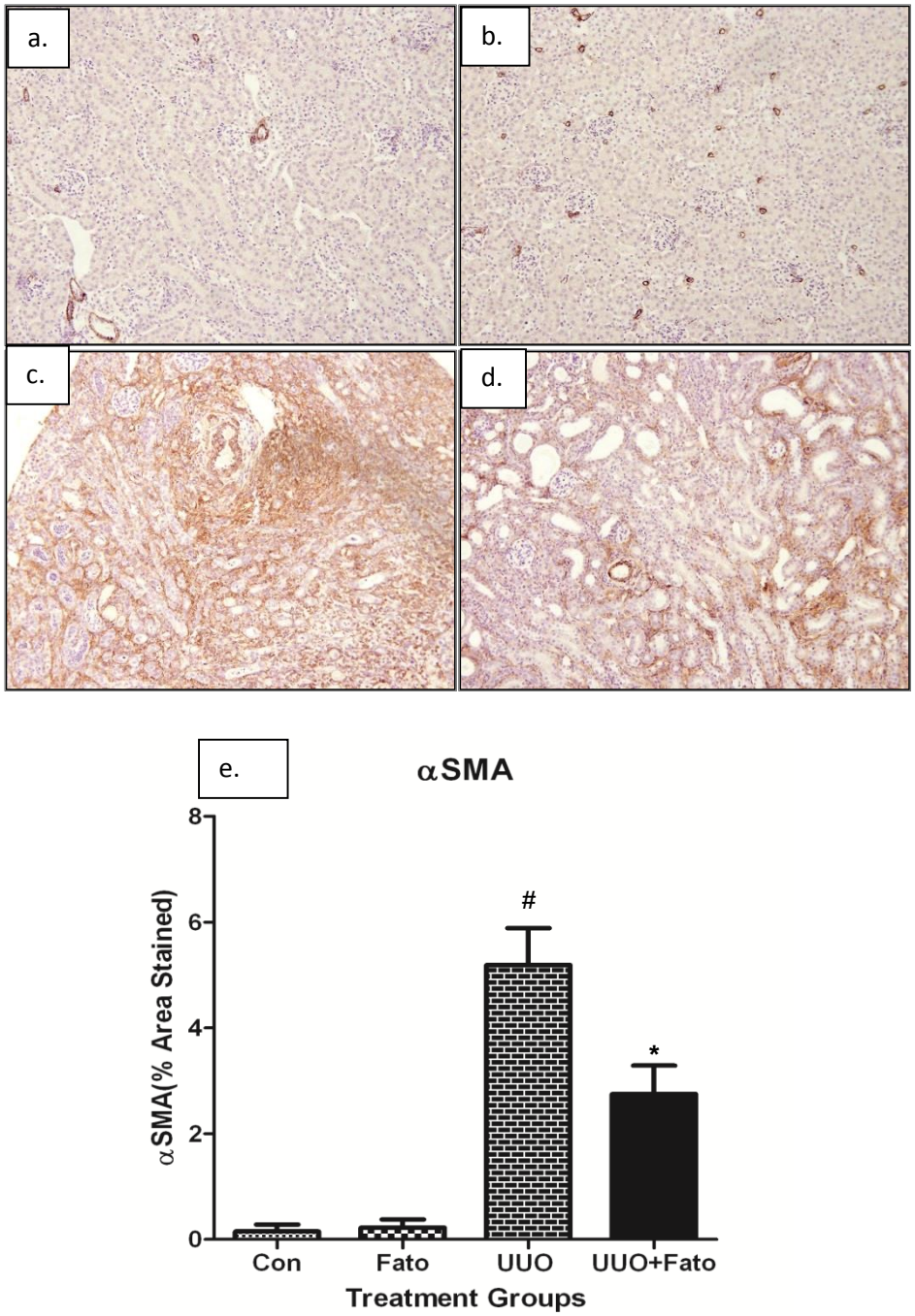

Figure 24: The amount of myofibroblast infiltration was evaluated by using its αSMA expression. (a) Control. (b) Fatostatin. (c) UUO. (d) UUO with fatostatin treatment. (e) The percentage of αSMA staining to the total area of tissue was evaluated in the 14day UUO mice and their respective controls. (Mean ±SEM; #p<0.0001 vs. Control; *p<0.05 vs. UUO; n=3 for controls; n=7 for UUO group)

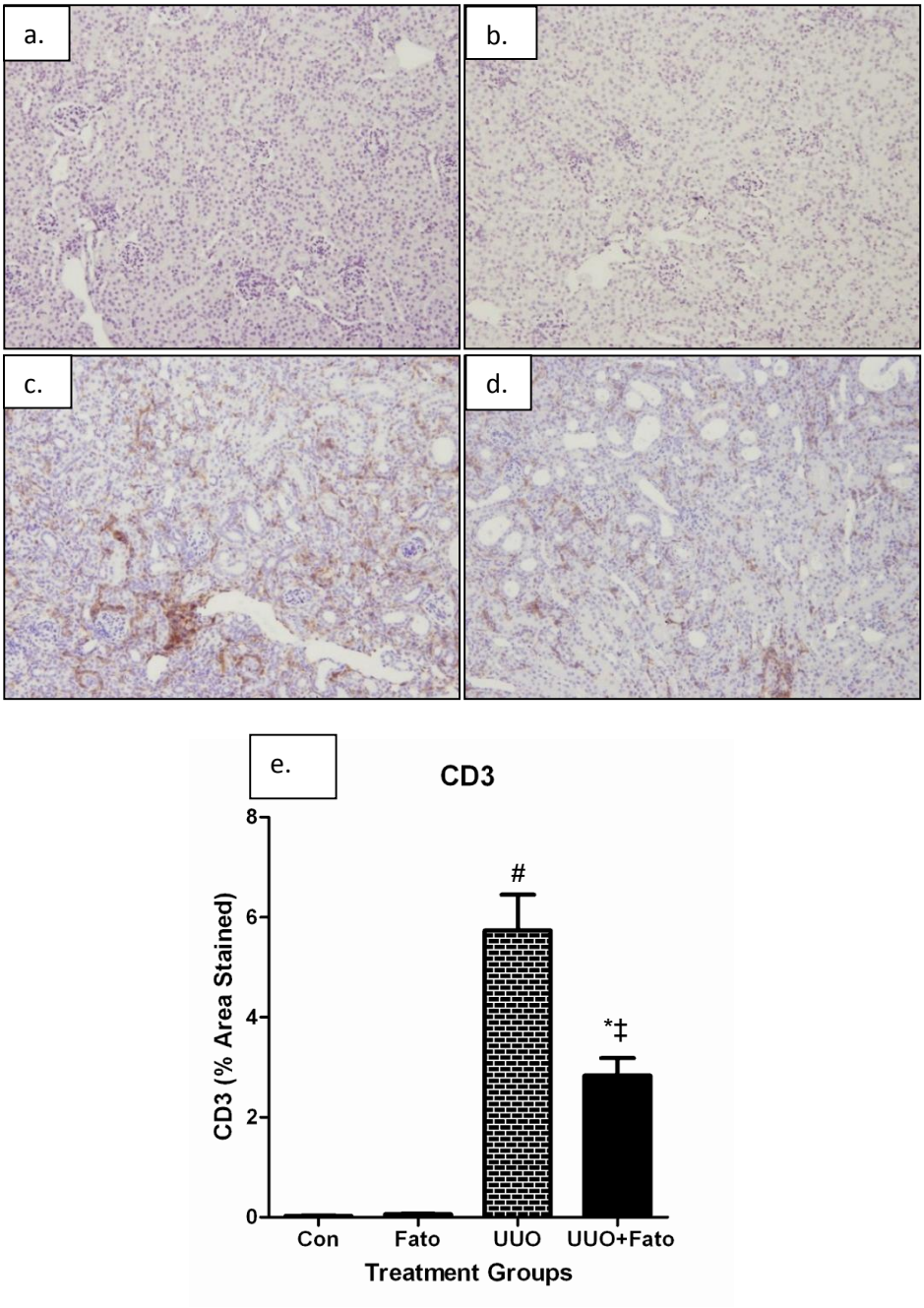

Figure 25: The amount of T-cell infiltration was evaluated sing its CD3 antigen expression. (a) Control. (b) Fatostatin. (c) UUO. (d) UUO with fatostatin treatment. (e) The percentage of CD3 staining to the total area of tissue was evaluated in the 14 day UUO mice and their respective controls (mean ±SEM; #p<0.0001 vs. Control; ‡p<0.05 vs. Fatostatin; *p<0.05 vs. UUO; n=3 for controls; n=7 for UUO group)

V Summary of Findings

Control vs. control fatostatin group

The controls were found to be similar in each group.

Control vs. 14-day UUO group

SREBP-1 and -2 were increased by UUO. The UUO group was found to have significantly higher staining for trichrome, PSR, fibronectin, αSMA and CD3. There was loss of proximal tubular mass and glomerulotubular integrity as assessed by lectin staining.

14-day UUO-fatostatin group vs. 14-day UUO group

Fatostatin decreased SREBP-1 and 2 expression. Fatostatin protected against the development of fibrosis as assessed by trichrome, PSR, and fibronectin staining. Fatostatin also decreased inflammatory cell infiltration, myofibroblast presence and preserved proximal tubular mass and glomerulotubular junctions.

VI Discussion

The understanding of tubulointerstitial fibrosis is critical to the development of an appropriate prevention technique to slow the progression of chronic kidney disease. In this study we have investigated the role of activated SREBP in response to TNFα and *in vivo* in a fibrotic kidney model. Activated SREBP was found to be upregulated in response to TNFα and to be dependent on both SCAP, S1P as well as caspase activity.

Since zVAD was able to inhibit SREBP-1 activation by TNFα, various caspases may be affecting this transcription factor. The possibilities include caspase 1 or 3, since both of these caspases have been found to lie upstream of SREBP-1. To investigate if caspase-3 is involved in this pathway, we used caspase-3 inhibitor VIII. This inhibitor targets and actively blocks the DEVD site commonly found on this caspase-3. The result is this caspase is no longer able to cleave PARP and therefore reduces the probability of the cell undergoing apoptosis. Interestingly blocking this site also resulted in reduced cleavage and thereby activation of SREBP-1. Caspase-3 cleaves the PARP between the aspartate and glycine residue, while it cleaves SREBP at aspartate and serine residue. There is a similarity in the cleavage location as one amino acid is found to be aspartate, while the other is a small amino acid. However this is just as hypothesis that needs to be further investigated.

Another way Caspase inhibition may be affecting SREBP is through pAkt. Recent literature found low levels of caspase-3 to cleave RasGAP into fragment N. Fragment N activates Akt, when the cell is under mild stress, to promote cell survival.

However when stress increases, fragment N is cleaved, unable to activate Akt. Therefore indirectly caspase-3 may be utilizing the SCAP mediated pathway to induce SREBP cleavage via S1P and S2P (Khalil et al., 2012). By utilizing inhibitors that target Akt, we disrupt the anterograde transport of SREBP from ER to Golgi and therefore reduce the amount of detected mature SREBP (Du et al., 2006). The study performed by Du et al., (2006) found that Akt co-localizes with GFP-SCAP, although they were not able to find any direct interactions. Another study found Akt to increase the stability of mSREBP-1 by inhibiting GSK2- dependent phosphorylation (Porstmann et al., 2008).

We also found that when we treated the cells with fatostatin, we reduced the amount of SREBP-1 cleavage, however, caspase-3 and PARP expression remained unaffected. This means that within the TNFα induced SREBP and apoptosis pathway, the caspase cleavage lies upstream of SREBP.

SREBP following its activation can induce apoptosis by binding to the SRE promoter (Higgins and Iannou, 2001). It is believed the activation of SRE genes is important to meet cholesterol deficit during apoptosis (Porter, 1999), as well as maintain the integrity of plasma membrane of the apoptotic cell (Wang et al., 1996). Another hypothesis states the requirement of cholesterol to assist in the scrambling of the plasma membrane when phosphotidylserine is externalized (Tepper et al., 2000). However these are just hypothesis and unfortunately due to time constraint, could not be tested in this study.

Using our findings from *in vitro* culture, we decided to use fatostatin in the UUO model to understand the importance of SCAP-mediated-SREBP activation in renal fibrosis and apoptosis. There is a large amount of literature showing high expression of TNFα in response to UUO (Docherty et al., 2006; Kaneto et al., 1996; Misseri et al., 2004). Since TNFα activates SREBP-1, we hypothesized that SREBP-1 may mediate some of its effects *in vivo*.

Fatostatin did not completely inhibit SREBP-1 upregulation in mice. This can potentially be the result of non-SCAP mediated upregulation of SREBP-1 that may be mediated by Caspase-3 or we may need a larger sample group to show significance. However we can only postulate as we have yet to evaluate the activation of this caspase, as well as its contribution to apoptosis.

We used TUNEL to investigate the number of cells undergoing apoptosis. We found the UUO group to have a larger number of apoptotic cells, indicating that suppressing the active SREBP may be beneficial for preventing apoptosis.

The lectin staining was found to be higher in the UUO-fatostatin group compared to UUO group. This shows that the glomerulotubular integrity was maintained more in the UUO-fatostatin group. The larger number of surviving PTEC were indicated in figure 17. This illustrates a larger number of tubular cells maintaining their lectin staining, therefore are still viable and functional.

As shown by others, we found UUO to induce fibrosis. This was associated with an increase in the number of infiltrating cells such as myofibroblast and T-cells. Since fatostatin attenuated these parameters, we conclude that active SREBP contributes to

renal fibrosis and injury. By inhibiting activation of this transcription factor, we may maintain the viability of nephrons.

The pathway as to how cells undergoing apoptosis induce fibrosis is intricate. When cells begin to undergo apoptosis, they leave behind space. This space needs to be filled so the surviving nephrons can have the support they need. Hence the necessity of fibrosis. The second reason as to why fibrosis develops is that tubular cells release cytokines such as TGFβ and CTGF. TGFβ is known to attract fibroblast and myofibroblast cells for healing purposes. Other cytokines are released that recruit and activate macrophages. Although macrophages could not be evaluated in our study due to technical reasons, they may play a great role in the observed TIF (Tian et al., 2006). Following engulfment of apoptotic cells, the activated macrophages increase their TGFβ synthesis and thereby increase fibroblast recruitment (Xiong et al., 2013). This would explain why the UUO group was found to have increased amount of ECM deposition. From these results, we find SREBP-1 plays a major role in the apoptotic and fibrotic response in the UUO model. Similarly T-cells are known to increase the amount of fibrocyte which also assist in accumulation of ECM (Niedermeier et al., 2009).

Our next step is to determine the pathway utilized by SREBP to regulate apoptosis and fibrosis. A simple pathway is illustrated below. In the future I would also like to assess the involvement of TGFβ in this pathway.

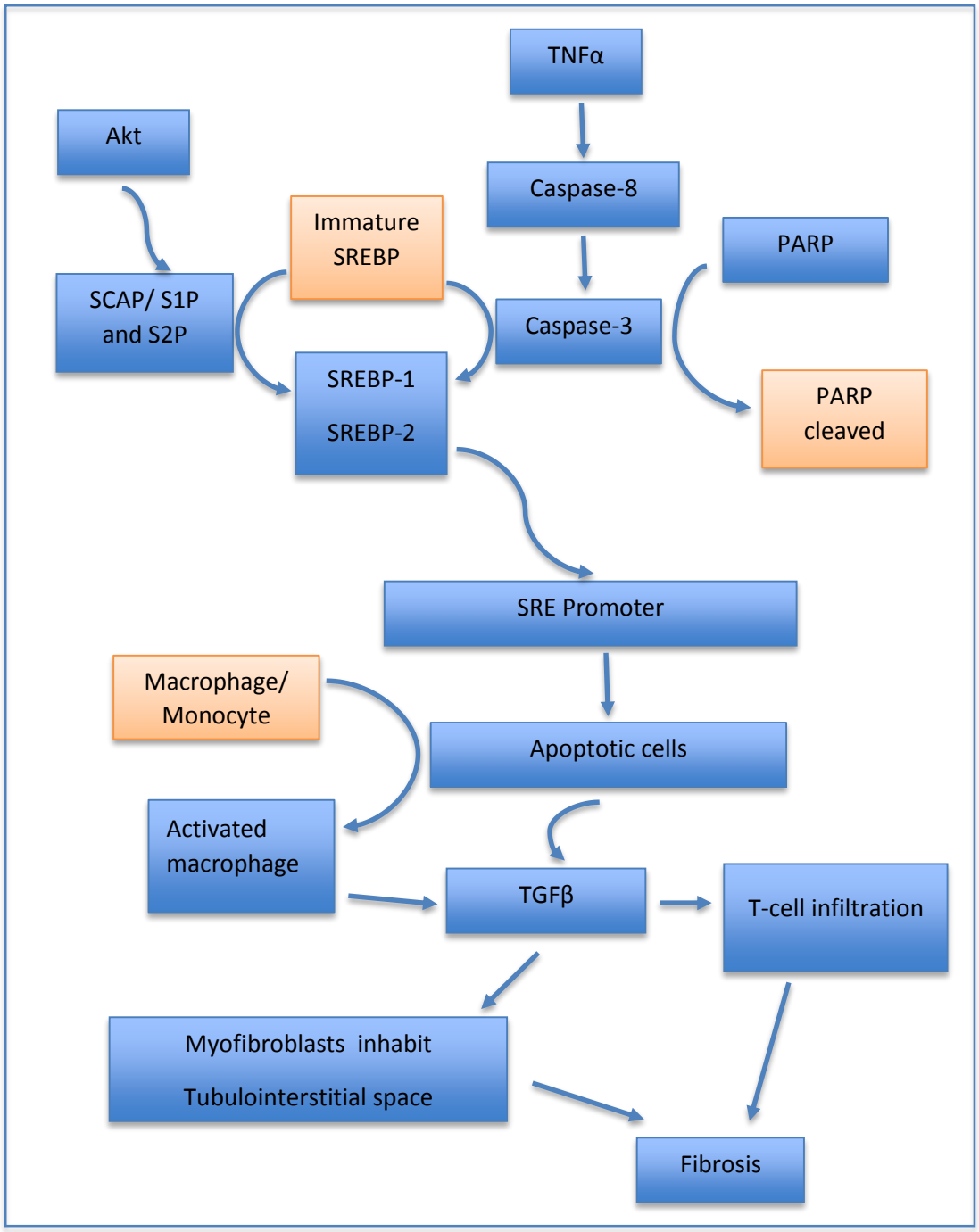
TNFα
Akt
Caspase-8
Immature SREBP
PARP
SCAP/ S1P and S2P
Caspase-3
SREBP-1
SREBP-2
PARP cleaved
SRE Promoter
Macrophage/ Monocyte
Apoptotic cells
Activated macrophage
TGFβ
T-cell infiltration
Myofibroblasts inhabit Tubulointerstitial space
Fibrosis

VII References

Ame, J-C., Rolli, V., Schreiber, V., et al., 1999. PARP-2 a novel mammalian DNA damage-depedent poly(ADP-ribose) polymerase. J. Biol. Chem. 274, 17860-8

Bechtel, W., McGoohan, S., Zeisberg, E et al., 2010. Methylation determines fibroblast activation and fibrogenesis in the kidney. Nat. Med. 16, 544-51

Boise, L.H., Thompson, C.B., 1997. Bcl-X_L can inhibit apoptosis in cells that have undergone Fas- induced protease activation. P. Natl. A Sci. 95, 3759-64

Bonventre, J., Yang, L., 2011. Cellular pathophysiology of ischemic acute kidney injury. J. Clin. Invesr. 121, 4120-221

Chevalier, E.R., 1996. Growth factors and apoptosis in neonatal ureteral obstruction. J.Am. Soc. Nephrol. 7, 1098-105

Chinnaiyan, A.M., O'Rourke, K., Tewari, M., et al., 1995. FADD, a novel death domain-containing protein, interacts with the death domain of Fas and initiates apoptosis. Cell 81, 505–12

Cohen, J.J., Duke, R.C., Fadok, V.A., et al., 1992.Apoptosis and programmed cell death in immunity. Annu. Rev. Immunol. 10, 267-93

Creasey, A.A., Doyle, L.V., Reynolds, M.T., et al., 1987. Biological effects of recombinant human tumor necrosis factor and its novel muteins on tumor and normal cell lines. Cancer Res. 47(1), 145-149..

Deng, Y., Ren, X., Yang, L., et al., 2003. A JNK-Ddependent pathway is required for TNFα-Induced Apoptosis. Cell 115 (1), 61-70.

Di, X., Kristiana, I., Wong, J., et al., 2006. Involvement of Akt in ER-to-golgi transport of SCAP/SREBP: a link between a key cell proliferative pathway and membrane synthesis. Mol Biol Cell 17, 2735-45

Docherty, N.G., O'Sullivan, O.E., Healy, D.A., et al., 2006. Evidence that inhibition of tubular cell apoptosis protects against renal damage and development of fibrosis following ureteric obstruction. Am. Physiol. Soc. 290, F4-13

Ellis, R.E., Yuan, J. and Horvitz, H.R., 1991. Mechanisms and functions of cell death. Annu Rev Cell Biol. Annu. Rev. Cell Biol. 7, 663-98.

Elmore, S., 2007. Apoptosis: a review of programmed cell death. Toxicol Pathol 35, 495-516

Forbes, M.S., Thornhill, B.A., Chevalier, R.L., 2011. Proximal tubular injury and rapid formation of atubular glomeruli in mice with unilateral ureter obstruction: a new look at an old model. Am. J. Physiol. Renal Physiol. 301, F110-7

Goldstein, J.L., Rawson, E.B., Brown, M.S., 2002. Mutant mammalian cells as tools to delineate the sterol regulatory element-binding-protein pathway for feedback regulation of lipid synthesis. Arch. Biochem. Biophys. 397, 139-48

Green, D.R., Reed, J.C., 1998. Mitochondria and apoptosis. *Science* 281, 1309-12.

Grone, H., Weber, K., Grone, E., et al., 1987. Coexpression of Keratin and Vimentin in damaged and regenerating tubular epiltelia of the kidney. Am J.Pathol. 129, 1-8

Hagimoto, N., Kuwano, K., Miyazaki, H., et al., 1997. Induction of apoptosis and pulmonary fibrosis in mice in response to ligation of Fas antigen. Am J Respir Cell Mol Biol 17, 272–78

Hengartner, M.O., 2000. Review article The biochemistry of apoptosis. Nature 407, 770-776

Higgins, M.E., Iannou, Y.A., 2001. Apoptosis-induced release of mature sterol regulatory element-binding proteins activates sterol-responsive genes. J. Lipid. Res. 42, 1939-46

Hong, S.J., Dawson, T.M., Dawson, V.L., et al., 2004. Nuclear and mitochondrial conversations in cell death: PARP-1 and AIF signaling. Trend. Pharmacol. Sci. 25 (5), 259-64

Hsu, H., Xiong, J., Goeddel, D.V., 1995. The TNF receptor 1-associated protein TRADD signals cell death and NFκB activation. *Cell* 81, 495–504.

Humphreys, B., Lin, S.L., Kobayashi, A., et al., 2010. Fate tracing reveals the pericyte and not epithelial origin of myofibroblasts in kidney fibrosis, Am. J. Pathol. 176, 85-97.

Kamisuki, S., Mao, Q., Abu-Elheiga, L., et al., 2009. A small molecule that blocks fat synthesis by inhibiting the activation of SREBP. Chem. Biol. 16, 882-92

Kim, J-S., He, L., Lemasters, J.J., 2003. Mitochondrial permeability transition" a common pathway to necrosis and apoptosis. Biochem. Bioph. Res. Co. 304, 463-70

Lin, S-L., Kisseleva, T., Brenner, D.A., et al., 2008. Pericytes and perivascular fibroblasts are the primary source of collagen-producing cells in obstructive fibrosis of the kidney. Am. J. Pathol. 173, 1617-27

Liu, W., Li, X., Zhao, Y., et al., 2013. Dragon (RGMb) inhibits E-Cadherin expression and induces apoptosis in renal tubular epithelial cells. Cell Biol. In press

Ishii, G., Sangai, T., Sugiyama, K., et al., 2005. In Vivo Characterization of Bone Marrow–Derived Fibroblasts Recruited into Fibrotic Lesions. Stem Cells. 23(5), 699-70

Iwano, M., Plieth, D., Danoff, T.M., et al., 2002. Evidence that fibroblasts derive from epithelium during tissue fibrosis. J Clin Invest 110, 341–50.

Kaissling, B., LeHir, M., Kriz, W., 2013. Renal epithelial injury and fibrosis. Biochem. et Bio. Acta. 1832, 931-9

Kaneto, H., Morrissey, J.J., McCracken, R., et al., 1996. The expression of mRNA for tumour necrosis factor-α increases in the obstructed kidney of rats soon after unilateral ureteral ligation. Nephrology 2 (3), 161-6.

Kaufann, S.H., Desnoyers, S., Ottaviano, Y., et al., 1993. Specific proteolytic cleavage of poly(ADP-ribose) polymerase: an early marker of chemotherapy-induced apoptosis. Cancer Res,. 53, 3976-85

Kennedy, W.A., Stenberg, A., Lackgren, G., et al., 1994. Renal tubular apoptosis after partial ureteral obstruction. J. Urol. 152 (2), 658-64

Khalil, H., Peltzer, N., Walicki, J., et al., 2012. Caspase-3 protects stressed organs against cell death. Mol. Cell. Biol. 32, 4523-33.

Kim, J.M., Eckmann, L., Savidge, T.C., et al., 1998. apoptosis of human intestinal epithelial cells after bacterial invasion. J Clin Invest 102, 1815-23

Koesters, R., Kaissling, B., Hir M.L., et al., 2010. Tubular overexpression if transforming growth factor-β induces autophagy and fibrosis and not mesenchymal transition of renal epithelial cells. Am. J. Pathol. 177, 632-43

Kothakota, S., Azuma, T., Reinhard, C., et al., 1997. Caspase-3 generated fragment of gelsolin: effector of morphological change in apoptosis. Science. 278, 294-8
Kriz, W., Hir, L., 2005. Pathways to nephron loss starting from glomerular disease-insights from animal models. Kidney Int. 67, 404-19.

Kriz, W., Kaissling, M., Hir, L., 2011. Epithlial-mesenchumal transition (EMT) in kidney fibrosis: fact of fantasy? Am. J. Pathol. 179, 2177-88.

Lan, R., Geng, H., Polichnowski, A., et al., 2012. PTEN loss defines a renal TGFβ induced tubule phenotype of faled differentiation and JNK signaling during renal fibrosis. Am. J. Physiol. Renal Physiol. 302, F1210-23

Larrick, J.W., Wright, S.J., 1990. Cytotoxic mechanisms of tumor necrosis factor-a. Faseb J. 4(14), 3215-23.

Lemaire, C., Andreau, K., Souvannavong, V., et al., 1998. Inhibition of caspase activity induces a switch from apoptosis to necrosis. Febs. Lett. 425, 266-70
Lhotak, S., Sood, S., Brimble, E., et al., 2012. ER stress contributes to renal proximal tubule injury by increasing SREBP-2-mediated lipid accumulation and apoptotic cell death. AJP - Renal Physiol 303 (2), F266-78

Liu, Y., 2012. Renal fibrosis: new insights into the pathogenesis and therapeutics. Kidney Int. 69, 213-17

Loetscher, H., Pan, Y.C., Lahm, H.W., et al., 1990. Molecular cloning and expression of the human 55Kd tumor necrosis factor trceptor. Cell 61, 351-9

Picard, N., Baum, O., Vogetseder et al., 2008. Origin of renal myofibroblast in the model of unilateral ureter obstruction in the rat. Histochem. Ce.. Biol. 130, 141-55

Misseri, R., Medrum, D.R., Dagher, P., et al., 2004. Unilateral ureter obstruction induces renal tubular cell production of tumor necrosis factor-alpha independent of inflammatory cell infiltration. J. Urol. 172, 1595-9

Misseri, R., Meldrum, D.R., Dinarelo, C.A., et al., 2005. TNF-alpha mediates obstruction-induced renal tubular cell apoptosis and proapoptotic signaling. Am. J. Physiol. Renal Physiol. 288, F406-11

Nicolson, D.W., ali, A., Thornberry, N.A., et al., 1995. Identification and inhibition of the ICE/CED-3 protease necessary for mammalian apoptosis. Natur.e 376, 37-43

Niedermeier, M., Reich, B., Gomez, M.R., et al., 2009. CD4+ T cells control the differentialtion of Gr1+ monocytes into fibrocytes. P Natl. Acad. Sci. 106, 17892-97

Ogasawara, J., Watanabe-Fukunaga, R., Adachi, M., et al., 1993. Lethal effect of the anti-Fas antibody in mice. *Nature* 364, 806-9.

Ortiz, A., C. Bustos, J., Alonso, R., 1995. Involvement of tumor necrosis factor-alpha in the pathogenesis of experimental, and human glomerulonephritis. Adv. Nephrol. Necker Hosp. 24, 53–77.

Pai, J.T., Brown, M.S., Goldstein, J.L., 1996. Purification and cDNA cloning of a second apoptosis-related cysteine protease that cleaves and activates sterol regulatory element binding proteins. P. Natl. A. Sci.

Parraga, A., CBellsolell, L., Derre-D'Amare, A.R., et al., 1998. Co-crystal struction of sterol regulatory element binding protein 1a at 2.3 A resolution. Strcture. 6, 661-72

Porstmann, T., Santos, C.R., Griffiths, B., et al., 2008. SREBP activity is regulated by mTORC1 and contributes to Akt-dependent cell growth. Cell Metab. 8, 224-36

Porter, A.G., 1999. Protein translocation in apoptosis. Trends. Cell. Biol. 9, 394-401

Postlethwaite, A.E., Keski-Oja, J., Moses, H.L., et al., 1987. Stimulation of the chemotactic migration of human fibroblast by transforming growth factor β. J. Exp. Med. 165, 251-6

Rishi, V., Gal, J., Krylov, D., et al., 2004. SREBP-1 dimerization specificity maps to both the helix-loop-helix and leucine zipper domains: use of a dominant negative. J. Biol Chem. 279, 11863-74

Roy, N., Deveraux, Q.L., Takahashi, R., et al., 1997. Recent diversification in African greenbuls (Pycnonotidae: Andropadus) supports a montane speciation model. EMBO J., 16 (23) (1997), p. 6914

Salvensen, G.S., Duckett, C.S., 2002. IAP proteins: blocking the road to death's door. Nat. Rev., Mol. Cell Biol., 3 (6), 401

Schall, T.J., Lewis, M., Koller, K.J., et al., 1990. Molecular cloning and expression of a receptor for human tumor necrosis factor. Cell 61, 362-70

Schreiber, V., Arme, J-C., Dolle, P., et al., 2002. Poly(ADP-ribose) polymerase-2 (PARP-2) is required for efficient base excision DNA repair in association with PARP-1 and XRCC1. J. Biol. Chem. 277,23028-36

Smeets, B., Boor, P., Dijkman, H., et al., 2013. Proximal tubular cells contain a phenotypically distinct, scattered cell population inovolved in tubular regeneration. J. Pathol. 299 (5), 645-59

Statistics Canada. Canadian Community Health Survey (CCHS). 2011. Web. 27.Aug. 2012. <http://www.statcan.gc.ca/tables-tableaux/sum-som/l01/cst01/health53a-eng.htm >

Strutz, F., Zeisberg, M., 2006. Renal fibroblasts and myofibroblasts in chronic kidney disease. J Am Soc Nephrol 17, 2992–8.

Sugarman, B.J., Aggarwal, B.B., Hass, P.E., et al., 1985. Recombinant human tumour necrosis factor-a: effects on proliferation of normal and transformed cells in vitro. Science 230(4728), 943-45.

Tepper, A.D., Ruurs, P., Wiedmer, T., et al., 2000. Sphingomyelin hydrolysis to ceramide during the execution phase of apoptosis results from phospholipid scrambline and alters cell-surface morphology. J. Cell Biol. 150, 155-64

Terzaghi, M., Nettesheim, P., William, M.L., 1978. Repopulation of denuded tracheal grafts with normal, preneoplastic and neoplastic epithelial cell populations. Cancer Res. 38, 4546–53.

Thornberry, N.S., Lazebnik, Y., 1998. Caspases: Enemies within. Science 281, 1312-6

Thornhill, B.A., Forbes, M.S., Marcinko, E.S., et al., 2007. Glomerulotubular disconnection in neonatal mice after relief of partial ureter obstruction. Kidney Int. 72, 1103-12

Tian, S., Ding, G., Jia, R., et al., 206. Tubulointerstitial macrophage accumulation is regulated by sequentially expressed osteopontin and macrophage colony-stimulating factor: implication for the role of atorvastatin. Mediators Inflamm. 2, 1-9

Tomooka, S., Border, W.A., Marshall, B.C., et al., 1992. Glomerular matrix accumulation is linked to inhibition of the plasmin protease system. Kidney Int. 42,

Uriarte, S.M., Joshi-Barve, S., Song, Z., et al., 2005. AKT inhibition upregulates FasL, downregulates c-FLIPs and induces caspase-8-dependent cell death in Jurkat T lymphocytes. Cell Death Differ. 12, 233-42

Wahl, S.M., Hunt, D.A., Wakefield, L.M., et al., 1987. Transforming growth factor type beta induces monocyte chemotaxis and growth factor production. Proc. Natl. Acad. Sci. USA 84, 5788-92

Wajant H., 2002. The Fas signaling pathway: more than a paradigm. *Science* 296, 1635-6.

Wang, L., Du, F., Wang, X., 2008. TNF-alpha induces two distinct caspase-8 activation pathway. Cell 133, 693-703

Wang, X., Zeleski, N.G., Yang, J., et al., 1996. Cleavage of sterol regulatory element binding proteins (SREBPs) by CPP32 during apoptosis. EMBO. J. 15, 1012-20

Whiteman, E.L., Cho, H., Birnbaum, M.J., 2002. Role of AKT/protein kinase B in metabolism. Trends Endocrinol. Metab. 13, 444-51

Xiong, W., Frash, S.C., Thomas, S.M., et al., 2013. Induction of TGF-β1 sunthesis by macrophage in response to apoptotic cells require activation of the scavenger receptor CD36. PLOS ONE 8(8), 1-12

Yu, S-W., Wang, H., Poitras, M.F., et al., 2002. Mediation of poly(ADP-ribose) Polymerase-1-dependent death by apoptosis-inducing factor. Science. 297, 259-63

Zeisberg, E.M., Tarnavski, O., Zeisberg, M., et al., 2007. Endothelial-to-mesenchymal transition contributes to cardiac fibrosis. Nat Med 13, 952–61.